

## General Disclaimer

### One or more of the Following Statements may affect this Document

- This document has been reproduced from the best copy furnished by the organizational source. It is being released in the interest of making available as much information as possible.
- This document may contain data, which exceeds the sheet parameters. It was furnished in this condition by the organizational source and is the best copy available.
- This document may contain tone-on-tone or color graphs, charts and/or pictures, which have been reproduced in black and white.
- This document is paginated as submitted by the original source.
- Portions of this document are not fully legible due to the historical nature of some of the material. However, it is the best reproduction available from the original submission.

N 66. 3.8.9.42.

FACILITY FORM 602

(ACCESSION NUMBER)	(THRU)
77	1
(PAGES)	(CODE)
CR-65532	14
(NASA CR OR TMX OR AD NUMBER)	(CATEGORY)

development  
research  
manufacture

components  
systems  
instruments

**BARNES ENGINEERING COMPANY**  
30 Commerce Road Stamford, Connecticut

GPO PRICE \$  
CFSTI PRICE(S) \$

Hard copy (HC) \$ 2.50  
Microfiche (MF) .75

ff 653 July 65

*Nasa CB 65532*

BEC PROJECT 3744

BARNES ENGINEERING COMPANY  
30 Commerce Road  
Stamford, Connecticut

LIBRARY COPY

SEP 20 1966

MANNED SPACECRAFT CENTER  
HOUSTON, TEXAS

ADDENDUM  
TO  
PHASE IA STUDY REPORT

Earth/Lunar Horizon Sensor Program

PREPARED BY:

*Frank Schwarz*  
Frank Schwarz  
Project Manager

*Thomas Falk*  
Thomas Falk  
Project Engineer

DATE: December 1, 1965

APPROVED BY:

*Frank Schwarz*  
Frank Schwarz  
Head, Advanced Development  
Department

*Robert W. Astheimer*  
Robert W. Astheimer  
Technical Director  
DEFENSE AND SPACE DIVISION

TABLE OF CONTENTS

	<u>Title</u>	<u>Page</u>
A1.	INTRODUCTION.....	A1-1
A2.	INDEXED EDGE TRACKERS.....	A2-1
A2.1	Indexing Movement.....	A2-1
A2.2	Single Detector, Linear Scan, Indexing.....	A2-5
A2.3	Field Switching, Five Thermistor Detectors, Indexing.....	A2-12
A2.4	Field Switching, Five Thermopile Detectors, Indexing.....	A2-24
A3.	SERVOED EDGE TRACKERS.....	A3-1
A3.1	Speed of Response.....	A3-1
A3.2	Field Switching Edge Tracker with Continuous Tracking Flat Mirror.....	A3-6
A3.3	Field Switching Edge Tracker with Servoed Optical Barrel.....	A3-16
A3.4	Field Switched Edge Tracker with Reflecting Prism Field Recombination.....	A3-19
A4.	ALL-ELECTRONIC EARTH/LUNAR HORIZON SENSOR SYSTEM	A4-1
A5.	CONCLUSIONS AND RECOMMENDATIONS.....	A5-1
A5.1	Field Switched Edge Tracking Horizon Sensors.....	A5-1
A5.2	Indexed Edge Tracking Horizon Sensors.....	A5-2
A5.3	All-Electronic Horizon Sensors.....	A5-3

LIST OF ILLUSTRATIONS

<u>Figure No.</u>	<u>Title</u>	<u>Location</u>
A2-1	Indexing Drive Block Diagram	Page A2-3
A2-2	Complementary Symmetry Flip-Flop	Page A2-4
A2-3	Single Detector, Linear Scan, Indexing	Page A2-6
A2-4	Method to Obtain Space Reference	Page A2-7
A2-5	Slot Geometry	Page A2-10
A2-6	Electronics Block Diagram with LVDT Reference Drive	Page A2-13
A2-7	Electronics Block Diagram with Pickup Coil Reference Drive	Page A2-14
A2-8	Scan with Torsional Fork	Page A2-15
A2-9	Optical and Electronics Drawing of Five Thermistor Indexed Edge Tracker	Page A2-16
A2-10	Detector Array Geometry	Page A2-19
A2-11	Optical Arrangement for 5-Element Thermopile Edge Tracker with Indexed Coarse Adjustment	Page A2-26
A2-12	Block Diagram for 5-Element Thermopile Edge Tracker with Indexed Coarse Adjustment	Page A2-26
A3-1	Edge Tracker Servo Block Diagram	Page A3-2

Illustrations (cont.)

<u>Figure No.</u>	<u>Title</u>	<u>Location</u>
A3-2	Optical Drawing of Field Switched Edge Tracker with Continuous Tracking Flat Mirror	Page A3-8
A3-3	Optical Drawing of Edge Tracker with Servoed Optical Barrel	Page A3-9
A3-4	Optical Drawing of Edge Tracker with Reflecting Prism Field Recombination	Page A3-10
A4-1	Optical Drawing of All-Electronic Multi-Element Thermopile Horizon Scanner	Page A4-6

LIST OF TABLES

<u>Table No.</u>	<u>Title</u>	<u>Location</u>
A2-1	Stepper Gear Motor Characteristics	Page A2-2
A2-2	BEC Five-Element Detector Array Characteristics	Page A2-18
A5-1	Comparison of Sensitivity, Accuracy, and Response Time of Various Horizon Sensor Systems	Page A5-5

## A1. INTRODUCTION

As a result of some uncertainty regarding response time requirements for the Earth/Lunar Horizon Sensor and the expectation that it would probably be higher than was thought some time ago, it has been suggested that Barnes Engineering Company reconsider the systems already described in the light of this possible requirement. It was also decided to include in this study report other possible systems which may be of interest and which offer some flexibility in the choice of response time.

At a recent conference between NASA/MSC technical personnel and BEC engineers, the question of response time was brought up. The exact system time constant requirement could not be specified at the time and numbers as demanding as 10 to 20 milliseconds were mentioned. However, it was thought more likely that a response time in the vicinity of one second would be the ultimate value. At this conference it was decided that Barnes Engineering Company would write an addendum to its Phase IA Study Report which would include trade-off considerations between time constant and accuracy and sensitivity for



the horizon sensor systems which merit further consideration. Also to be included were systems in which the coarse position of the planet horizon is acquired and determined by an indexing mechanism (operated only during acquisition and when large errors or altitude changes are encountered) and a fine position determining detector arrangement which is capable of fast response. NASA/MSC agreed to use the time interval in order to study and resolve the time constant requirement for the horizon sensor system.

The discussion below will be concerned with both new systems and with some of the horizon scanner systems discussed in the main body of the Phase IA report which are capable of performing the desired function within the accuracy requirements stated as the design goal and which will also provide some flexibility in the choice of response time in the range of values which may be required.

Our preference and recommendation, as will be discussed in some detail in later pages, continues to rest with the field switched edge tracker which was found in the Phase IA Study Report to offer the greatest advantages in virtually all

of the design goal considerations. The configuration which will be shown below--using a vibrating vane field switching method in lieu of the chopper motor arrangement--offers a wide latitude in the choice of response time in addition to a high reliability and adequate sensitivity and accuracy. The sensitivity and accuracy are naturally dependent on the response time requirements and improve for a system which can use a longer integration time. However, even for a system with a possible 20 millisecond response time requirement, this type of horizon sensor is believed to be capable of exceeding the design goals for accuracy and sensitivity. Moreover, we still believe that an engineering model of this type of system can be built within the schedule which was originally agreed to--a 2-month detail design study followed by an 8-month effort of design, fabrication, and testing of the engineering model.

## A2. INDEXED EDGE TRACKERS

A2-1 Indexing Movement

The same mechanism could be incorporated in all design concepts based on indexing. One degree steps with a precision better than  $\pm 0.025^\circ$  will be required, 20 in total: 10 and 10 on either side of a nominal center. The stepping movement will be reversible and will consume less than 1 watt power, including the losses in the control circuitry.

Such performance could be achieved, for example, with a permanent magnet gear stepper motor manufactured by the Vernitron Corporation. The characteristics are given in Table A2-1. A block diagram of the indexing system is given in Figure A2-1.

It will be noted that the motor, after a  $\pm 10^\circ$  movement, will be stopped electrically rather than by mechanical stops on the geared-down output shaft, since the torque needed to stop the motor (inertia reduced to the output shaft:  $0.15 \times (84.46)^2 = 1060 \text{ gm cm}^2$ ) is considerable.

The selection of circuits for control functions will be such as to minimize the average power consumption. An example is given in Figure A2-2. This is a complementary symmetry flip-flop with negligible power consumption in its off state.

TABLE A2-1

Stepper Gear Motor Characteristics

Manufacturer	Vernitron Corporation, Farmingdale, New York
Type Number	08MPB-AD4-AOGH90
Output Shaft Step Angle	1.07 degree
Gear Head Ratio	84.46:1
Maximum Unloaded Stepping Rate	50 steps per second
Stall Torque	0.25 oz. in.
Rotor Inertia	0.15 gm-cm <sup>2</sup>
Number of Phases	Four
Power Input	28 volts DC, 0.5 watt maximum
Operating Temperature	-20°C to +70°C
Size	2.5 inch overall length, 0.75 inch diameter

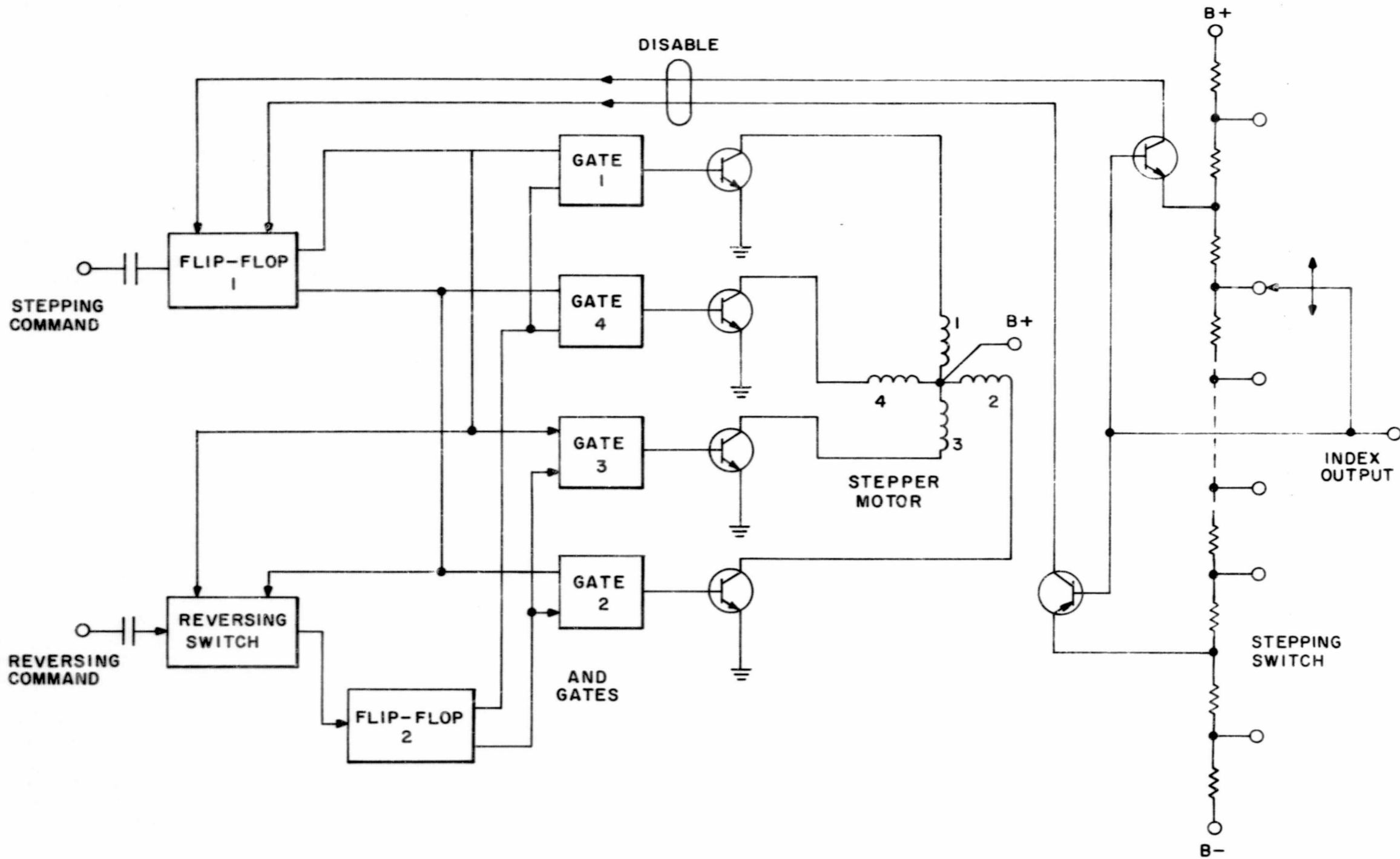


Figure A2-1 INDEXING DRIVE BLOCK DIAGRAM

21790

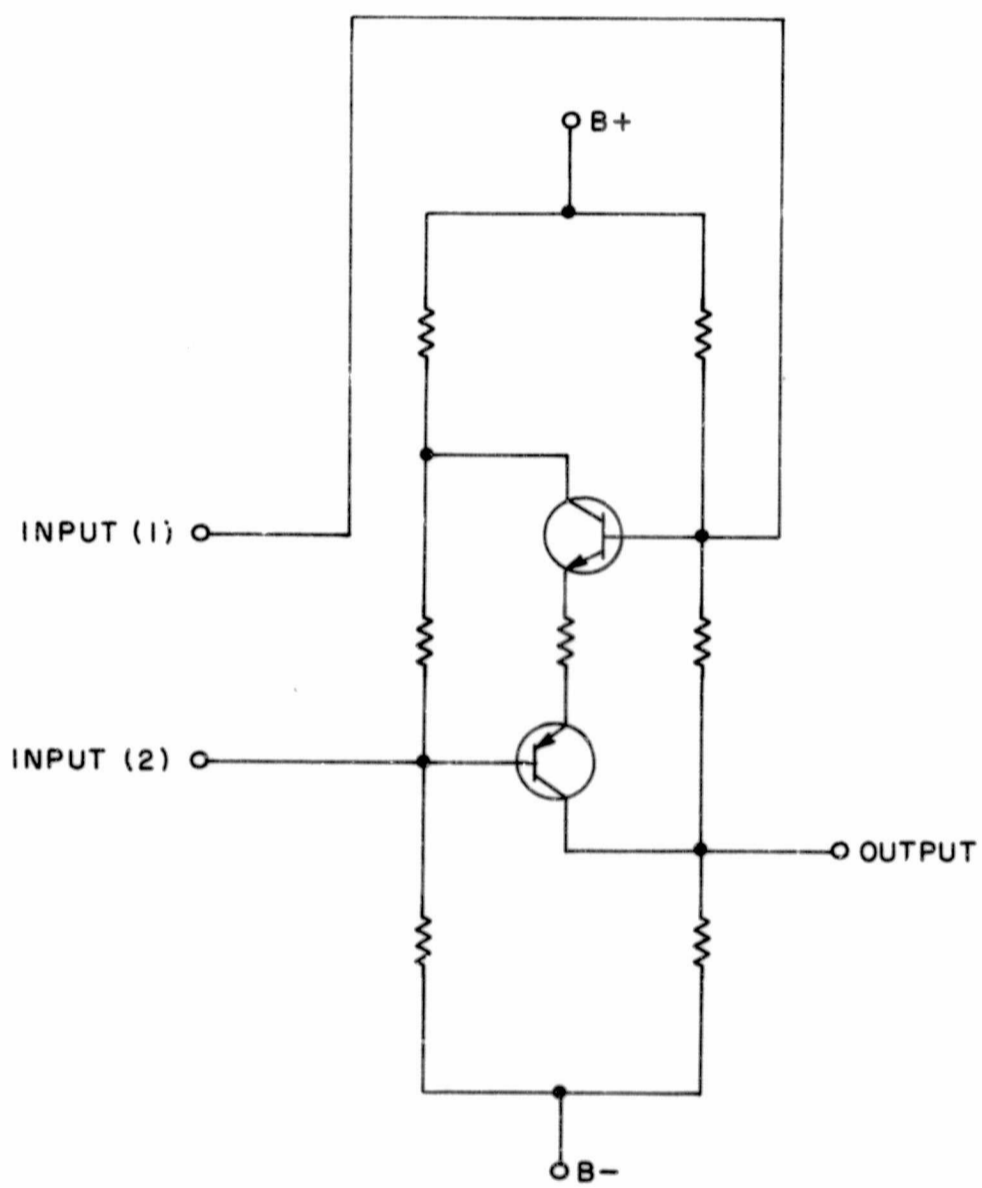


Figure A2-2 COMPLEMENTARY SYMMETRY FLIP-FLOP 21791

A2.2 Single Detector, Linear Scan, Indexing

(a) General - Let the line of sight of a detector be determined by the intersection of slots in two vanes mounted at an angle of about  $90^\circ$  with respect to each other on the two tines of a tuning fork (Figure A2-3). The line of sight will move along a straight path when the vibration of the fork causes the overlap of the two vanes to vary in a harmonic motion. Horizon crossover will be marked by a step in the detector output. The instant at which this step occurs has to be related to the motion of the tuning fork, thus locating the line of sight of horizon crossover with respect to the tuning fork mount. As is shown in Figure A2-4, we will arrange the system in such a way that the detector will not only trace a line perpendicular to and in the vicinity of the horizon but will compare this with a similar line in space (say  $10^\circ$  from the horizon) so as to continuously reference to space and to prevent possible cloud lock-on.

The precise determination of the instantaneous position of the vanes or the slots cut in the vanes could be accomplished by measuring the output of an electro-mechanical

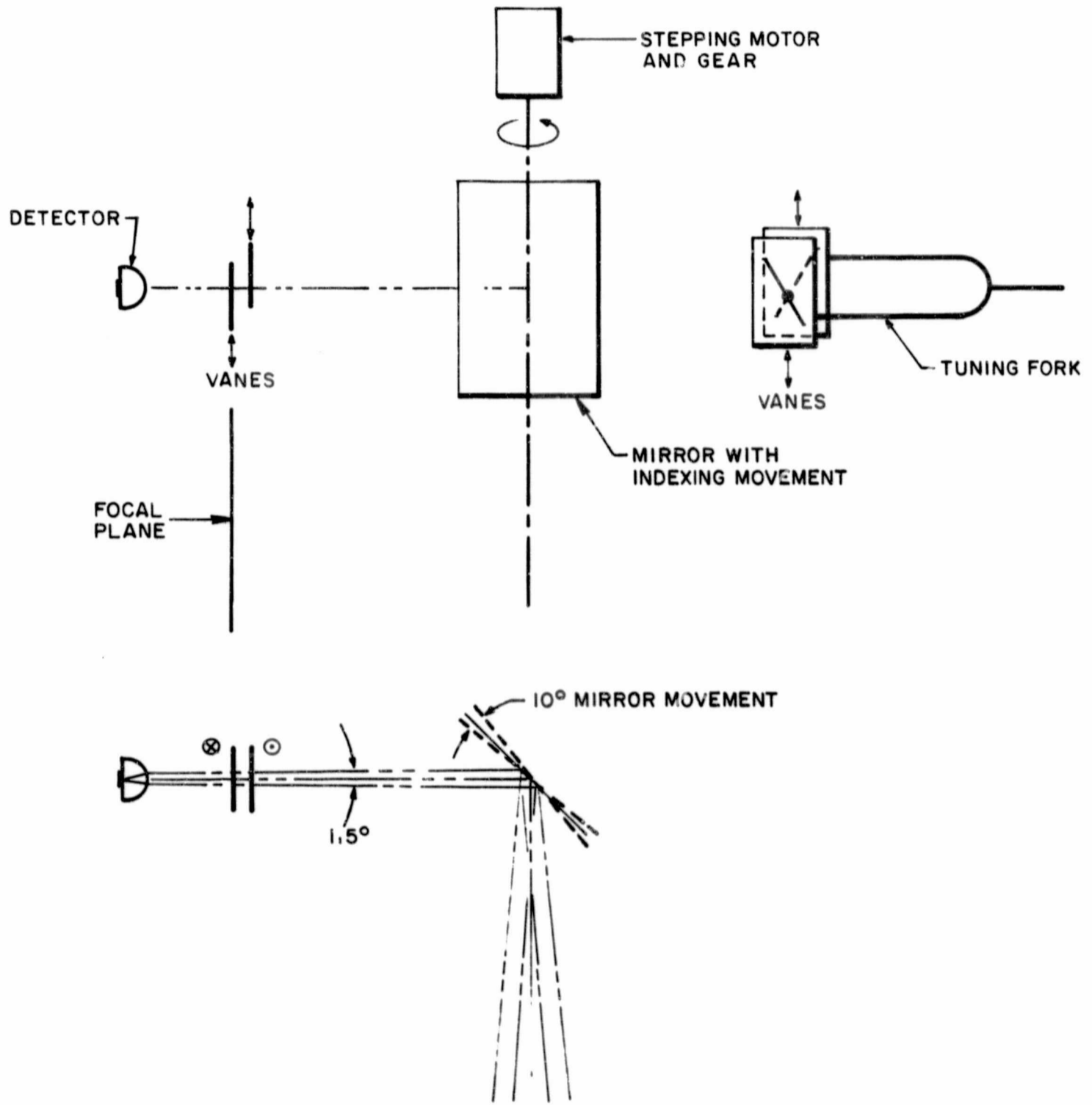


Figure A2-3 SINGLE DETECTOR, LINEAR SCAN, INDEXING



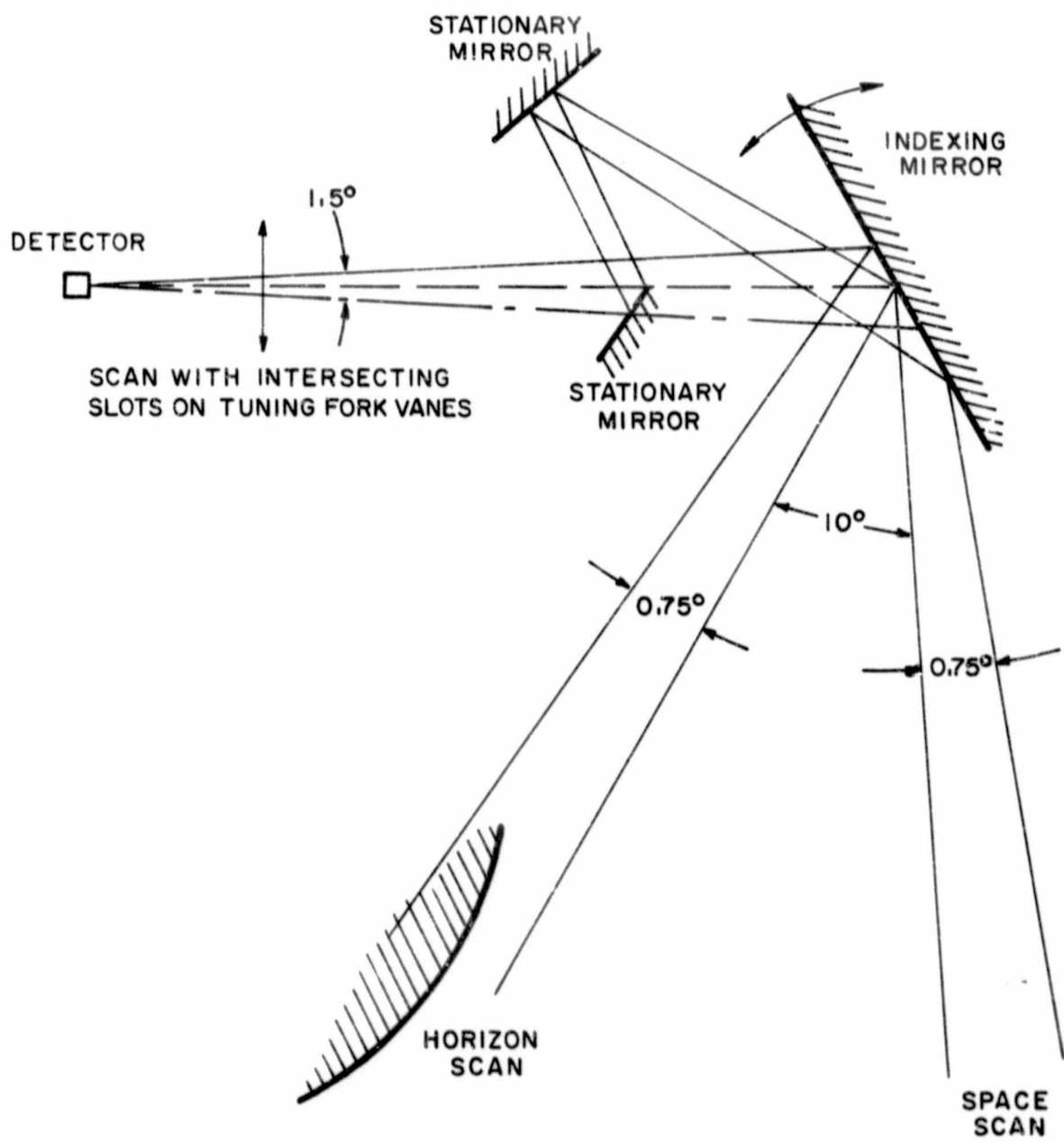


Figure A2-4 METHOD TO OBTAIN SPACE REFERENCE

transducer connected with the motion of the tuning fork. The transducer could be a differential transformer or a moving plate capacitor excited by a high frequency a.c. source. The motion of the fork amplitude modulates the output of the transducers. The demodulated output is a direct measure of the instantaneous displacement of the tuning fork. It is read out at the time when the detector output shows a step change. When the readout exceeds a set limit (corresponding to a one degree displacement), it will bring about a one degree indexing step in the direction determined by the polarity of the readout. The system output is a combination of the indexing readout and the transducer readout.

(b) System Parameters - For a 10 millisecond output response time, the rate of vibration of the tuning fork should be at least 100 cps. With a line of sight movement of  $1.5^\circ$  and the need for a modulation envelope smooth enough to resolve a displacement of 0.1 degree, the minimum frequency of transducer excitation is 3 kc. In order to obtain a smooth output function with this resolution, an excitation frequency of 15 kc should be chosen.

Consider the geometry of the intersection of the vanes that determines the field of view of the detector. If it is desired to achieve a given angular deflection of the line of sight with a minimum of tuning fork movement (about 2 millimeters for a  $1.5^\circ$  peak-to-peak movement), then the angle of the two slots (Figure A2-5) should be near  $90^\circ$ . This limits the ratio of the field of view dimensions parallel and perpendicular to the horizon. Thus both the field of view and the detector will tend to be square rather than a rectangle elongated in the ratio of 5:1 as with the edge tracker configurations described on pages 3-89 through 3-92 in the main body of the Phase IA study. This will reduce the signal-to-noise ratio calculated there by a factor of  $\sqrt{5}$ . Another reduction factor is due to the wider bandwidth of the system presently described. The 10 millisecond response time as compared to the 5 seconds assumed on page 3-92 modifies the signal-to-noise ratio calculated there by  $\sqrt{500}$ . Thus the signal-to-noise ratio for slicing at the 0.1 degree level in the present configuration is

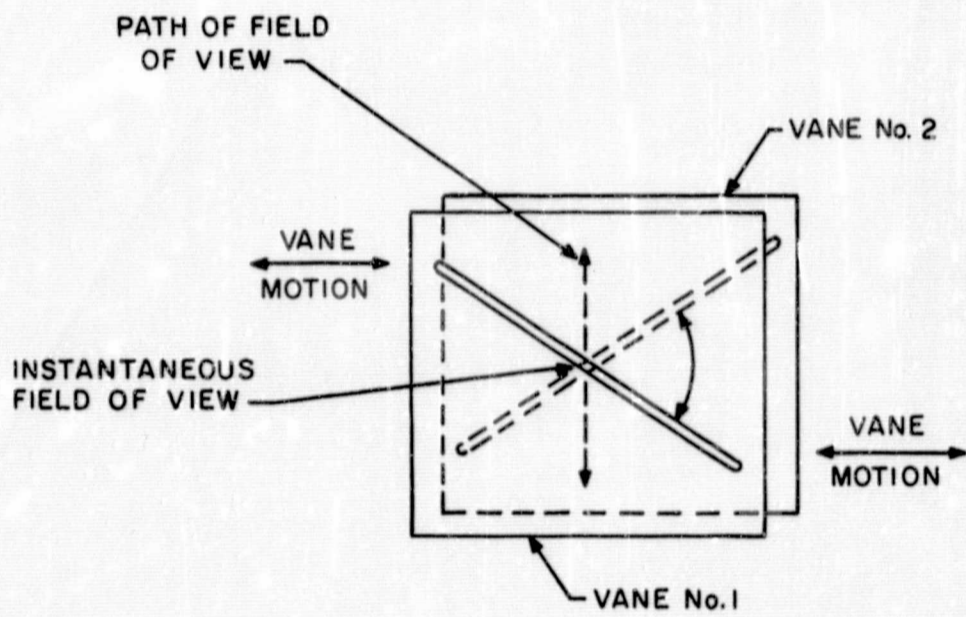


Figure A2-5 SLOT GEOMETRY

21794

$$30 \times \frac{1}{\sqrt{5 \times 500}} = 0.6$$

for the 90°K moon. Thus it turns out that in order to obtain a 5:1 signal-to-noise ratio for a 90°K moon the system speed of response would have to be reduced to give a response time of 700 milliseconds. It may be desired to increase the amount of energy received by the detector by using a wide and rectangular field of view. This would require a larger tuning fork movement (about 5 mm peak-to-peak oscillation). By this means, a S/N ratio of 5:1 could be achieved with a system response time of about 300 milliseconds. In order to obtain a system with still faster response time (e.g., 20 msec), it would be further necessary to greatly increase the diameter of the optics.

The system is not sensitive to small changes in the amplitude of the tuning fork motion, as the transducer would measure the actual deflection.

Instead of a transducer it may be possible to derive position information from the pickup coil of the tuning fork oscillator itself. The temperature stability of this arrangement

should be investigated. It would certainly obviate the need not only for a separate transducer but also for a high frequency source.

Two electronic block diagrams are given. The diagram of Figure A2-6 makes use of a differential transformer. In Figure A2-7, the pickup coil of the tuning fork is used for position reference.

The indexing output could be obtained either from a potentiometer or from a voltage divider network through a set of contacts actuated by the indexing mechanism (see Figure A2-1). The choice should be based on reliability considerations.

Similar system performance could be achieved with a scanning mirror mounted on a tuning fork with torsional vibrations (Figure A2-8). With this mechanism, a search mode could be implemented simply by increasing the amplitude of the tuning fork vibrations. Circular or elliptical scans can also be realized by coupling two torsional tuning forks  $90^\circ$  out of phase.

### A2.3 Field Switching, Five Thermistor Detectors, Indexing

This system employs a tuning fork to alternate the field of view of five thermistor detectors equally spaced in a linear array between two directions  $10^\circ$  apart (Figure A2-9).

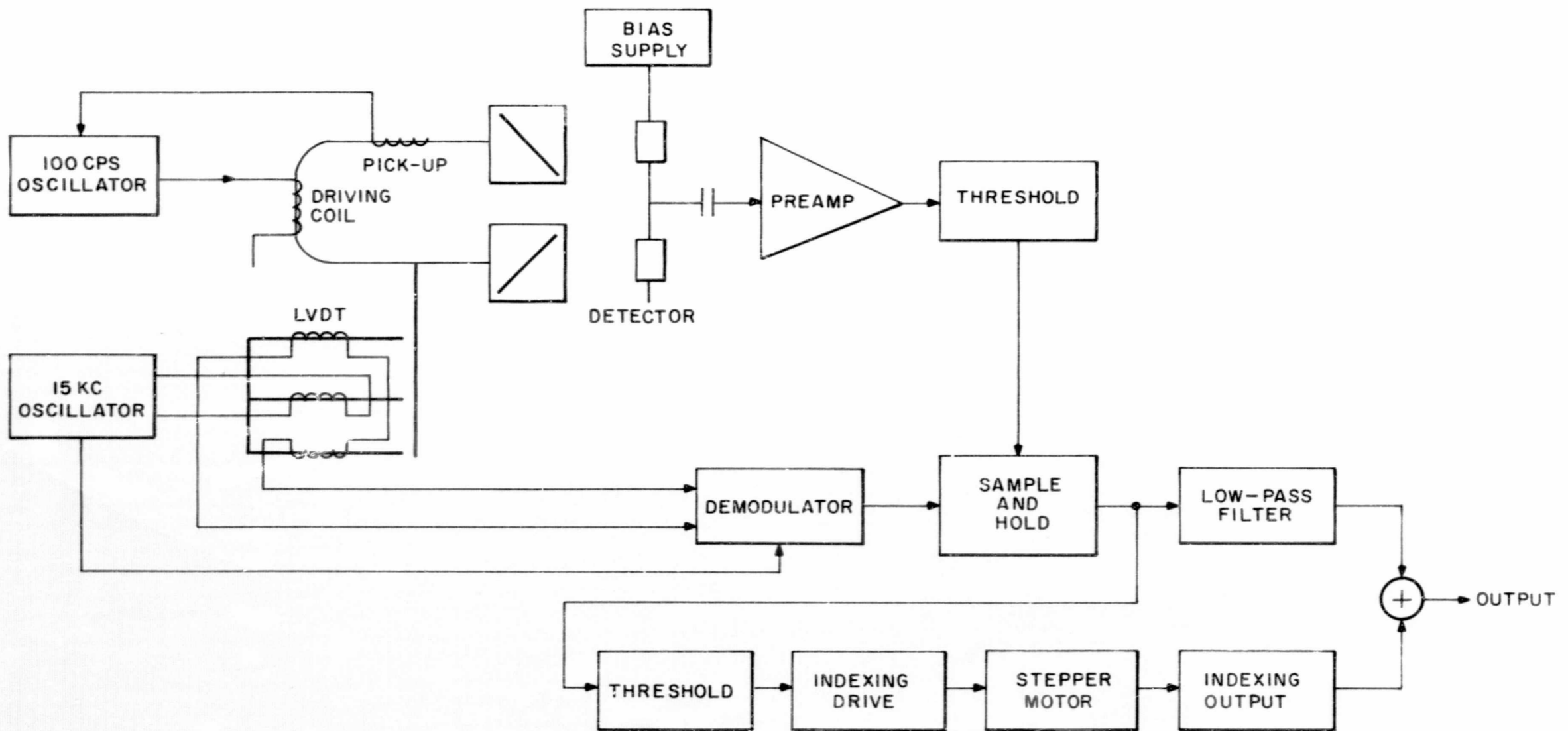


Figure A2-6 ELECTRONICS BLOCK DIAGRAM WITH LVDT REFERENCE DRIVE

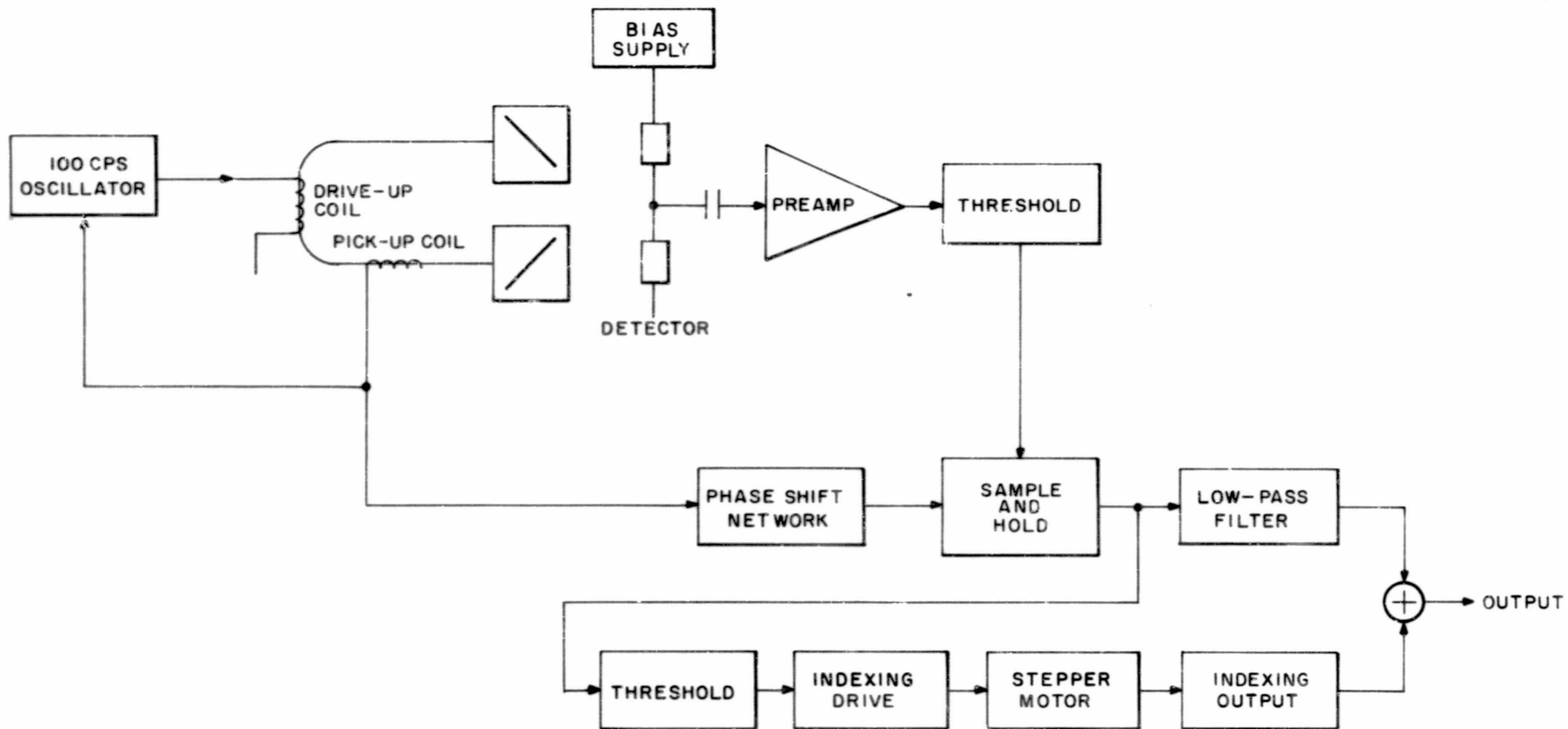
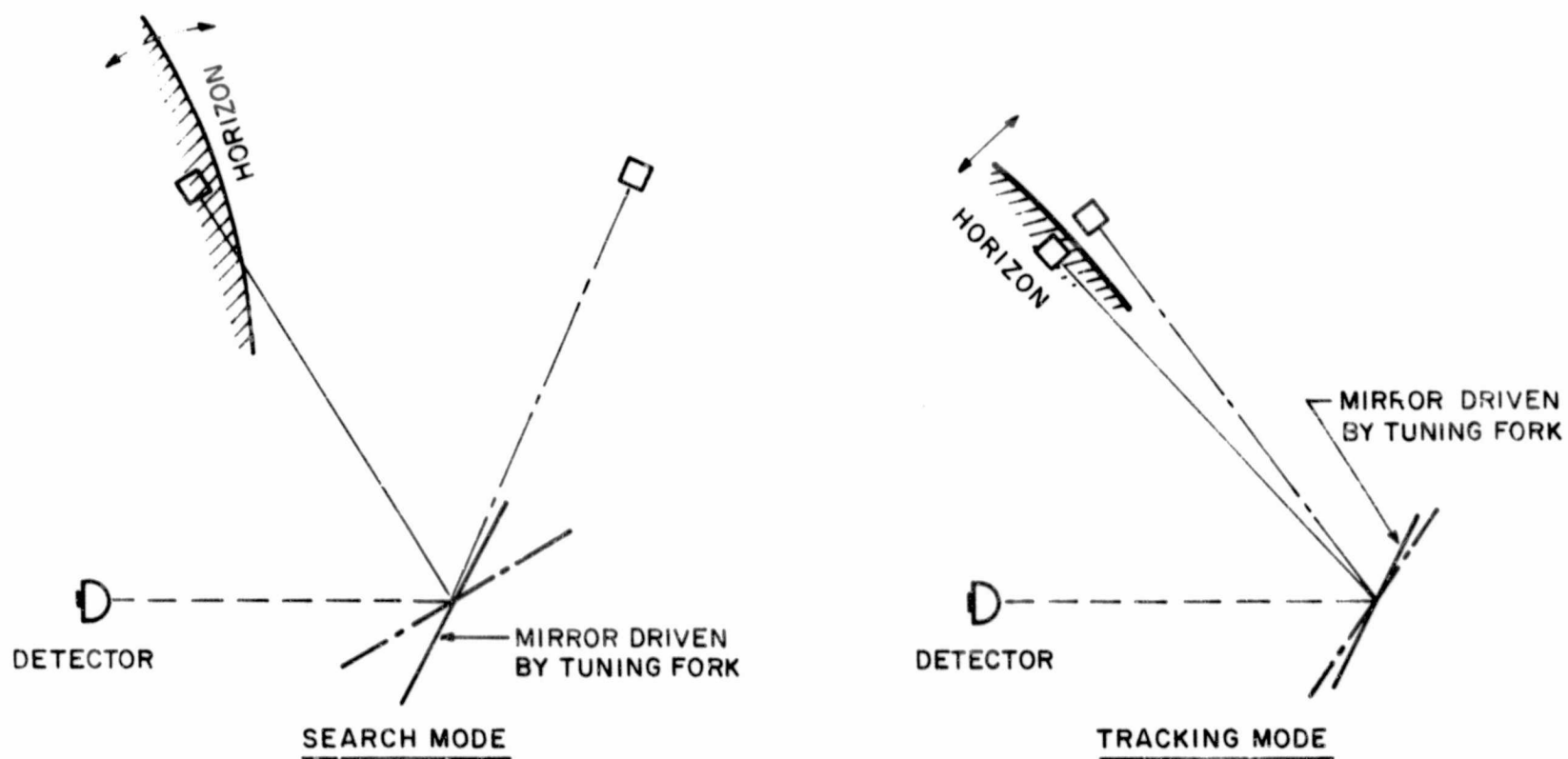


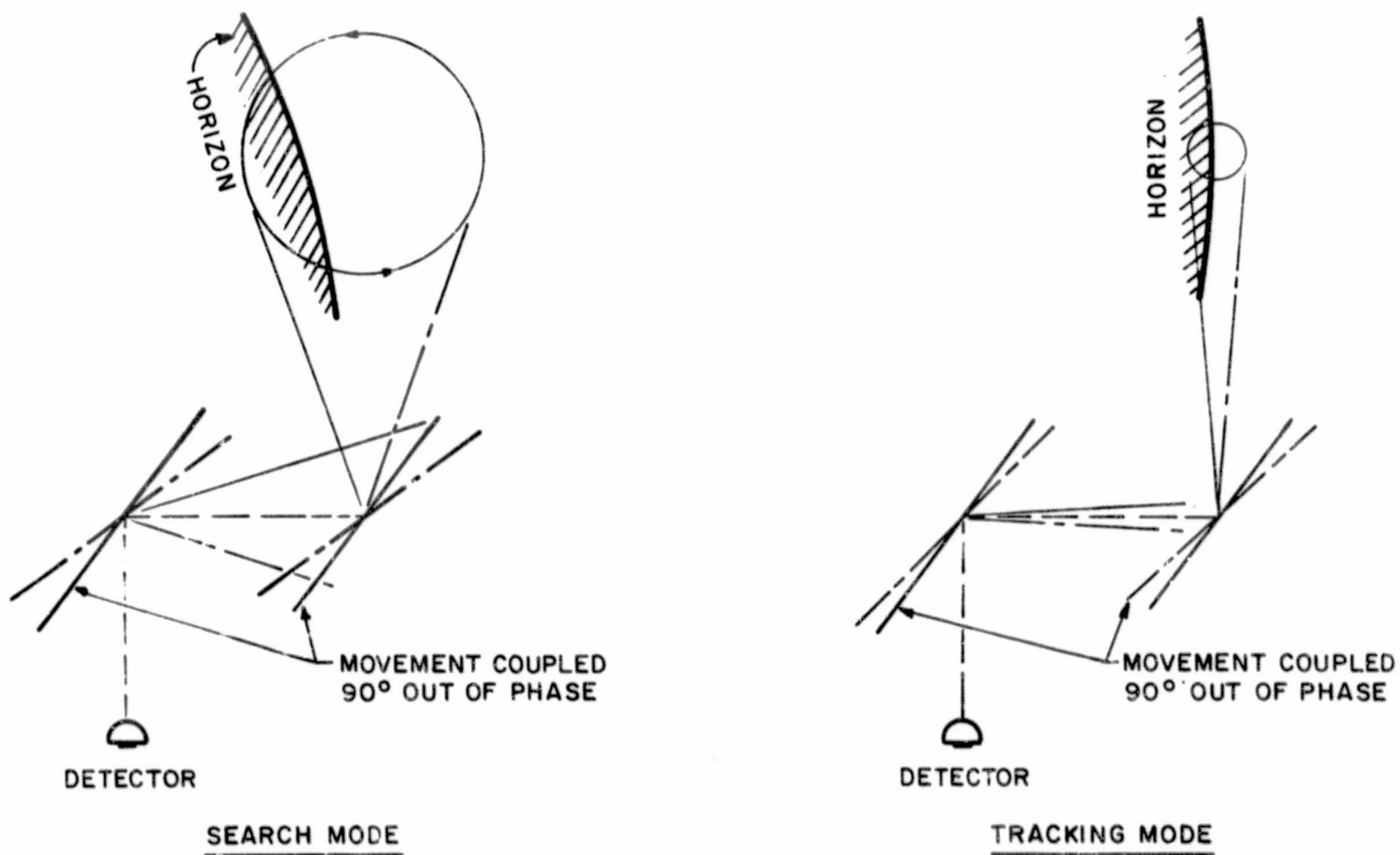
Figure A2-7 ELECTRONICS BLOCK DIAGRAM WITH PICK-UP COIL REFERENCE DRIVE

21796





LINEAR SCAN



CIRCULAR (OR ELLIPTICAL) SCAN

Figure A2-8 SCAN WITH TORSIONAL FORK

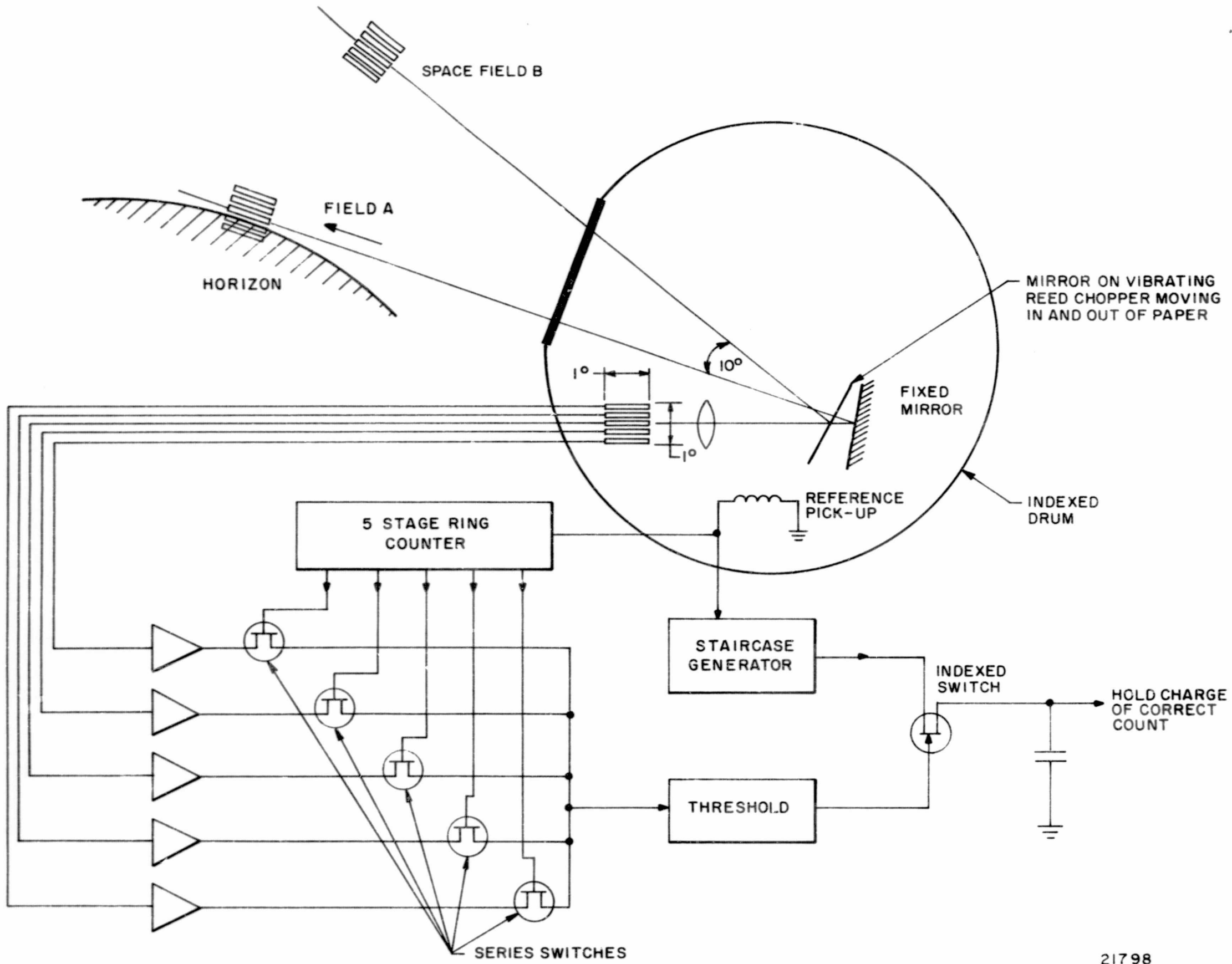


Figure A2-9 OPTICAL AND ELECTRONICS DRAWING OF 5 THERMISTOR INDEXED EDGE TRACKER

Interrogation of each of the five detectors determines the position of the horizon with a  $\pm 0.1^\circ$  accuracy if present within the  $1^\circ$  beam subtended by the array in direction A. If not present or if the horizon is about to leave the  $1^\circ$  beam, an indexing movement of one degree (or more if necessary) takes place.

Table A2-2 lists some of the characteristics of such an array of active thermistor flakes designed and built at Barnes Engineering Company.

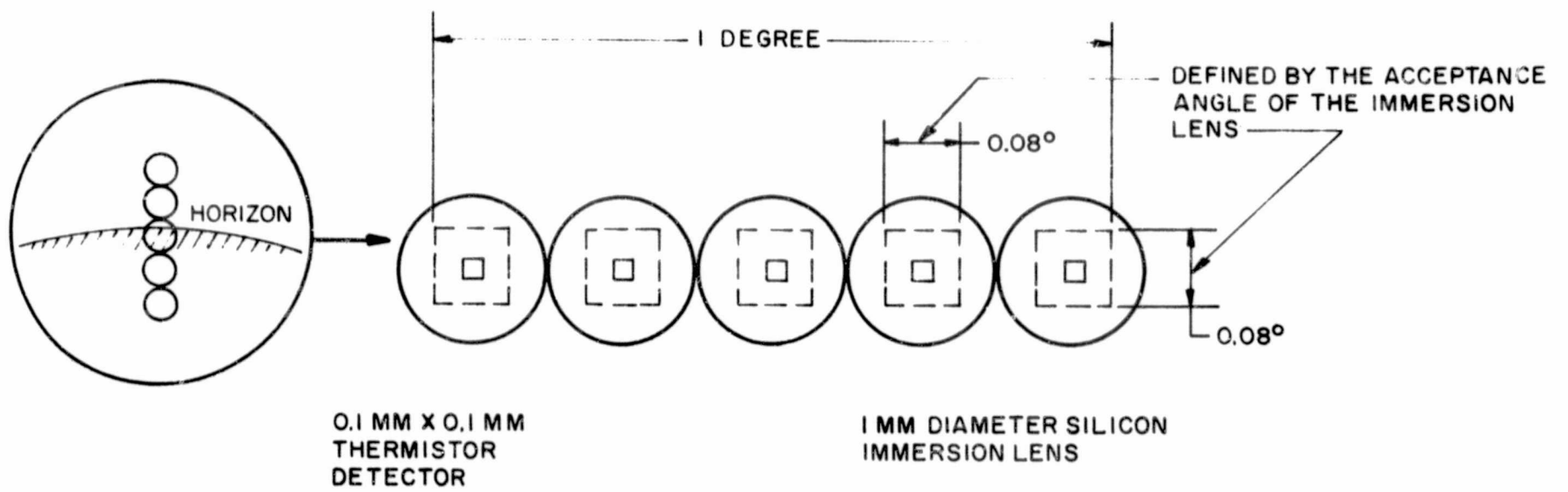
The geometry of the array in its present design is shown in part (a) of Figure A2-10. If the entire length of the array subtends one degree of arc, then the fields of view of the individual elements are limited to about  $0.08 \times 0.08$  degrees due to the 37 degree acceptance angle of the immersion lens.

For the present application, an increase of field of view and consequently higher signal-to-noise ratio could be achieved with one of the modified array geometries represented in parts (b) and (c) of Figure A2-10. By placing the array at an angle as shown in Figure A2-10b, we can reduce the separation of individual elemental fields of view (dotted lines) and, if desired, make the fields contiguous.

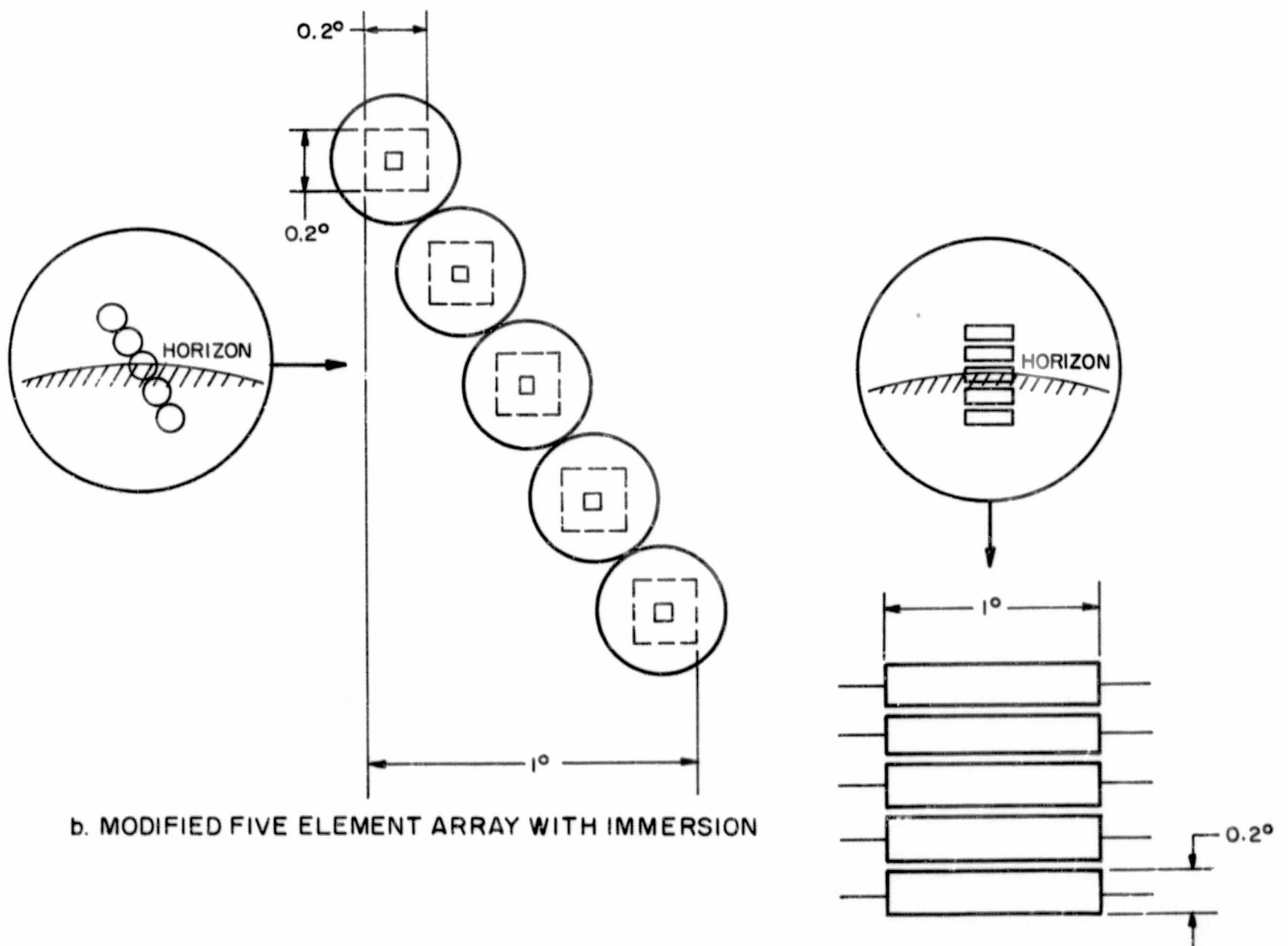
TABLE A2-2

BEC Five-Element Detector Array Characteristics

Detector Size	0.1 x 0.1 mm square
Separation Between Flakes	1 mm
Immersion	1 mm diameter silicon or germanium hemisphere
Flake Resistance	1 megohm
Bias Voltage	±40 volts
Responsivity	4000 volts/watt (500°K source, 15 cps chop)
Relative Responsivity Between 18-32μ	70% (combined figure with silicon immersion lens)
Time Constant	2 milliseconds



a. FIVE ELEMENT ARRAY IN ITS PRESENT FORM



b. MODIFIED FIVE ELEMENT ARRAY WITH IMMERSION

c. MODIFIED FIVE ELEMENT ARRAY, NO IMMERSION

Using the configuration according to part (b) of Figure A2-10, calculate the signal of any of the five detectors (connected in a bridge with its own compensating flake).

The radiant power incident on the detector is:

$$P_D = \Delta N \epsilon A_o \omega$$

For a portion of the moon surface at a temperature of 90°K and an optical passband between 20 $\mu$  and 40 $\mu$ :

$$\Delta N = 4 \times 10^{-5} \frac{\text{watt}}{\text{cm}^2 \text{ steradian}}$$

Assume an optical efficiency of 0.6 for the 20-40 $\mu$  optical filter:

$$\epsilon = 0.6$$

The area of a 2-inch diameter collector:

$$A_o = 20.2 \text{ cm}^2$$

The field of view of each detector of the five-element array with its own hemispherical immersion is 0.2 $^\circ$  x 0.2 $^\circ$ .

$$\omega = 12.3 \times 10^{-6} \text{ steradians}$$

A2 - 21

$$\begin{aligned} P_D &= 4 \times 10^{-5} \times 0.6 \times 20.2 \times 12.3 \times 10^{-6} \\ &= 60 \times 10^{-10} \text{ watt peak-to-peak variation} \\ &\text{or } 30 \times 10^{-10} \text{ watt peak variation} \end{aligned}$$

The ideal noise equivalent power of the detector:

$$NEP_o = 6.3 \times 10^{-10} \sqrt{A/\tau}$$

The detector area:  $0.1 \times 0.1 = 0.01 \text{ mm}^2$

The detector time constant: 2 milliseconds

$$NEP_o = 0.445 \times 10^{-10} \text{ watts} / \sqrt{\text{cps}} \text{ rms}$$

The following factors will deteriorate this figure:

- (1) The preamplifier noise figure, estimated at 2 db at 100 cps: 1.26.
- (2) With a 100 cps field of view alternation, the response of the 2 millisecond time constant detector will be down by:

$$\sqrt{1 + \frac{(100)^2}{\left[ \frac{(10^3)}{(2 \times 2\pi)} \right]^2}} = \underline{1.61}$$

(3) Detector bridge factor (the resistance of the compensating flake is not current driven): 1.41.

(4) Bias reduction for safe high temperature operation: 1.4.

$$\text{Total Deterioration: } 1.26 \times 1.61 \times 1.41 \times 1.4 = 4$$

$$\text{NEP} = 4 \times \text{NEP}_0 = 1.8 \times 10^{-10} \text{ w}/\sqrt{\text{cps}}$$

Thus the peak signal to rms noise in a 1 cps bandwidth:

$$\frac{30 \times 10^{-10}}{1.8 \times 10^{-10}} = 16.7$$

With a peak-to-rms ratio of 2.5 assumed for the noise, a 16 cps preamplifier bandwidth necessary for a 10 millisecond output signal rise time, and synchronous demodulation of the approximately sinusoidal signal, the signal-to-peak-noise ratio:

$$\frac{S}{N} = 16.7 \times \frac{1}{2.5} \times \frac{1}{\sqrt{16}} \times 0.636 = 1.06$$

To get a 5:1 signal-to-noise ratio without going to very bulky optics, it is necessary to reduce the bandwidth.



Let us assume it will be necessary to increase the output signal rise time to 100 milliseconds. The effect of this is threefold: it allows a low frequency (10 cps field alternation, it narrows the required preamplifier bandwidth to 1.6 cps, and on the other hand the lower frequency operation will somewhat worsen the preamplifier noise figure (from 2 to 3 db). The combined effect is:

$$\frac{1.61}{1.01} \times \sqrt{\frac{16}{1.6}} \times \frac{1.26}{1.41} = 4.5$$

The sensor provides at its output a signal-to-peak-noise ratio of:

$$1.06 \times 4.5 = 4.8 \text{ to } 1 \text{ for a } 90^\circ\text{K moon surface}$$

For a  $100^\circ\text{K}$  moon, the signal-to-peak-noise ratio is 7.6:1.

An outline of the electronics is contained in Figure A2-9.

Similar results could be obtained with a five-element unimmersed detector configuration (as shown in Figure A2-10c) which can have a much larger lateral subtense but does not have the advantage of optical gain through immersion.

It should be mentioned that the signal-to-noise ratios could be improved by about 25% if, instead of conventional

synchronous demodulation (multiplication by a square wave), multiplication by an in-phase reference sine wave were used. This could be done in a balanced FET multiplier as described by Highleyman and Jacob.<sup>1</sup>

#### A2.4 Field Switching, Five Thermopile Detectors, Indexing

In order to provide the desired accuracy and resolution with a horizon sensor system having no moving parts, it is necessary to use a large number of detectors and complex low-level switching circuitry, as is discussed in Section A4. A simpler system can be made, using a smaller number of detector elements which may be sampled at a predetermined rate and which need cover only a small portion of the total acquisition field while an indexing mechanism takes care of the larger changes in position. While the system does include a moving part in the form of an indexing mechanism, this device is seldom actuated, and therefore should have long life and should require virtually no electrical power, except when it is actuated.

---

<sup>1</sup>W. Highleyman and E. Jacob. "An Analog Multiplier Using Two Field Effect Transistors," IRE Transactions on Communication Systems, Vol. CS-10, pp. 311-317, September 1962.

Actuation is required only when there is a substantial change in altitude of the vehicle or when there is a large attitude error. The indexing mechanism in this case may be made to operate in steps of one degree while a five-element thermopile array resolves the field of view with small enough steps to extract the necessary error data with an accuracy of  $0.1^\circ$ .

The optical schematic is shown in Figure A2-11. In this drawing we show a spherical primary reflector and concentrically mounted thermopile detectors. In addition to the five thermopiles required for resolution at the edge of the planet, a single off-axis detector will be used to view an equivalent field placed away from the planet's edge and serving as a space reference.

An offset heat source will be required for this system to insure that all detectors viewing space are illuminated in such a way that their net outputs including the reference junctions will be zero volts. This offset heat source system (described in the paper listed as reference 12 in the Phase IA report) will avoid difficulties which may arise from any differences in responsivity between groups of thermopile detectors. A block diagram of the system is shown in Figure A2-12.

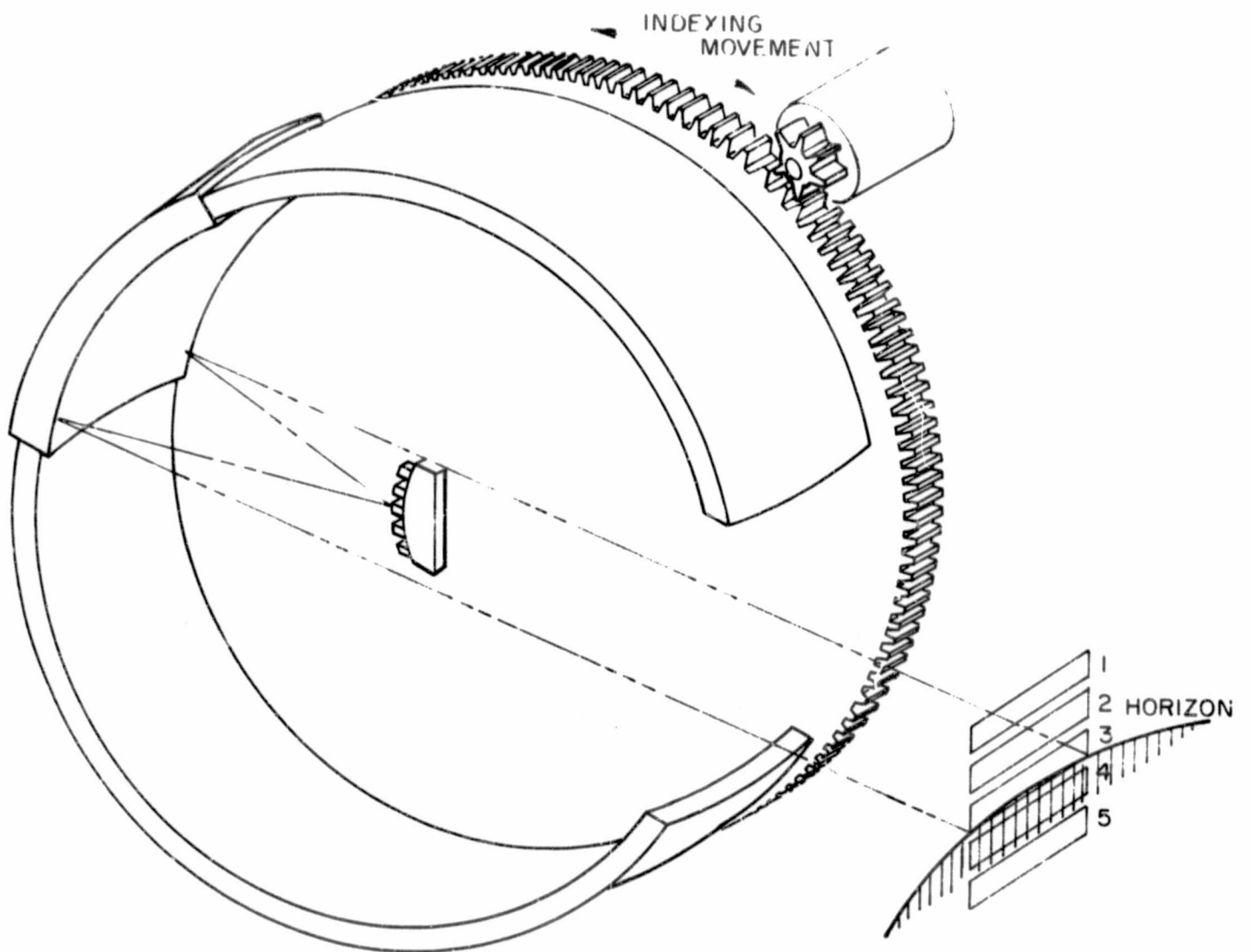


Figure A2-11 OPTICAL ARRANGEMENT FOR 5 ELEMENT THERMOPILE EDGE TRACKER WITH INDEXED COARSE ADJUSTMENT.

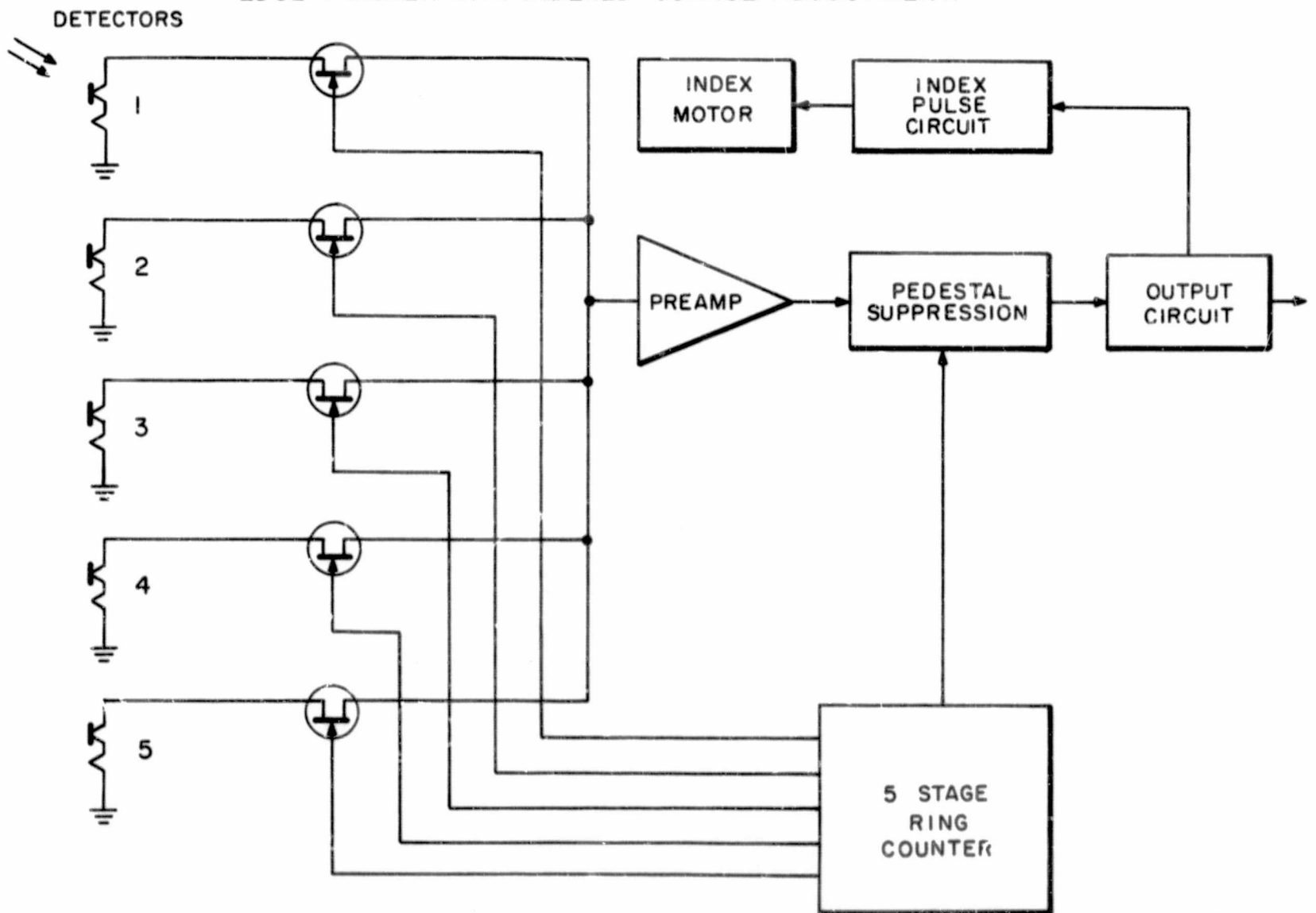


Figure A2-12 BLOCK DIAGRAM FOR 5 ELEMENT THERMOPILE EDGE TRACKER WITH INDEXED COARSE ADJUSTMENT.

The detectors to be used will be made of bismuth tellurium junctions. In this system, one might use 21 junction rectangular thermopiles located at the focus of a 2-inch diameter, f/0.7 reflecting spherical collector.

The sensitivity of such a system for 90°K lunar use is computed below:

Specific responsivity of 21-element  
bismuth tellurium thermopiles:  $R' = 25 \text{ volt/watt/cm}^2$

Time constant of detector = 100 milliseconds

Resistance of detector = 20,000 ohms

System noise (in 10 cps bandwidth) = 1 microvolt including  
thermal drift

Effective collector area,  $A_0 = 10 \text{ cm}^2$

Assume field of view =  $0.2^\circ \times 10^\circ$

$\omega = 0.0035 \times 0.175 = 6 \times 10^{-4} \text{ steradians}$

Effective radiance,  $\Delta N_{100^\circ\text{K}} = 10^{-4} \text{ in } 20\text{-}40\mu \text{ region}$

$$\begin{aligned} \text{Power on detector, } P_D &= \Delta N \omega A_O = 10^{-4} \times 6 \times 10^{-4} \times 10 \\ &= 6 \times 10^{-7} \text{ watts} \end{aligned}$$

$$A_D = \frac{\pi \times (0.25)^2}{4} = 0.05 \text{ cm}^2$$

$$\text{NEP} = \frac{A_D 10^{-6} \text{ V/w}}{25 \text{ V/cm}^2} = \frac{50 \times 10^{-6} \times 10^{-3}}{25} = 2 \times 10^{-9} \text{ watts/cycle}$$

$$\frac{S}{N} = \frac{6 \times 10^{-7}}{2 \times 10^{-9}} = 300$$

For 10 cps noise bandwidth and a factor of two for amplifier noise and rectification loss, the signal/noise becomes:

$$\frac{S}{N_{\text{rms}}} = 50 \quad \text{or} \quad \frac{S}{N_{\text{p-p}}} = 10$$

Note that, regardless of the sampling rate used in integrating the thermopiles, the time constant of the detector (100 msec) would limit the system response time. A faster responding detector would have lower responsivity and would require a larger bandwidth with consequent reduction of signal-to-noise ratio. Furthermore, while the instantaneous response

A2 - 29

may be adequate, we would still obtain a stepped or digital output rather than a desirable smooth, continuous response.

### A3. SERVOED EDGE TRACKERS

#### A3.1 Speed of Response

In this section we will concern ourselves with response time capabilities of the servoed edge tracker. The simplified block diagram of this system is given in Figure A3-1.

A<sub>1</sub> is a factor dependent on the optical design and detector sensitivity. It has dimensions of microvolt/degree.

A<sub>2</sub> is the total gain of the electronics from the detector output to the torquer drive. It is affected by a simple high frequency roll-off characterized by  $\tau_{amp}$  set by system noise considerations.

A<sub>3</sub> is the steady state output speed (in degrees per second) to input voltage ratio of the torque motor (friction losses neglected). It is affected by a time constant  $\tau_{torquer}$  determined by the torquer sensitivity (oz. in./amp), d.c. resistance, total inertia, and back emf.

A<sub>4</sub> is the scale factor of the output potentiometer driven by the torquer.



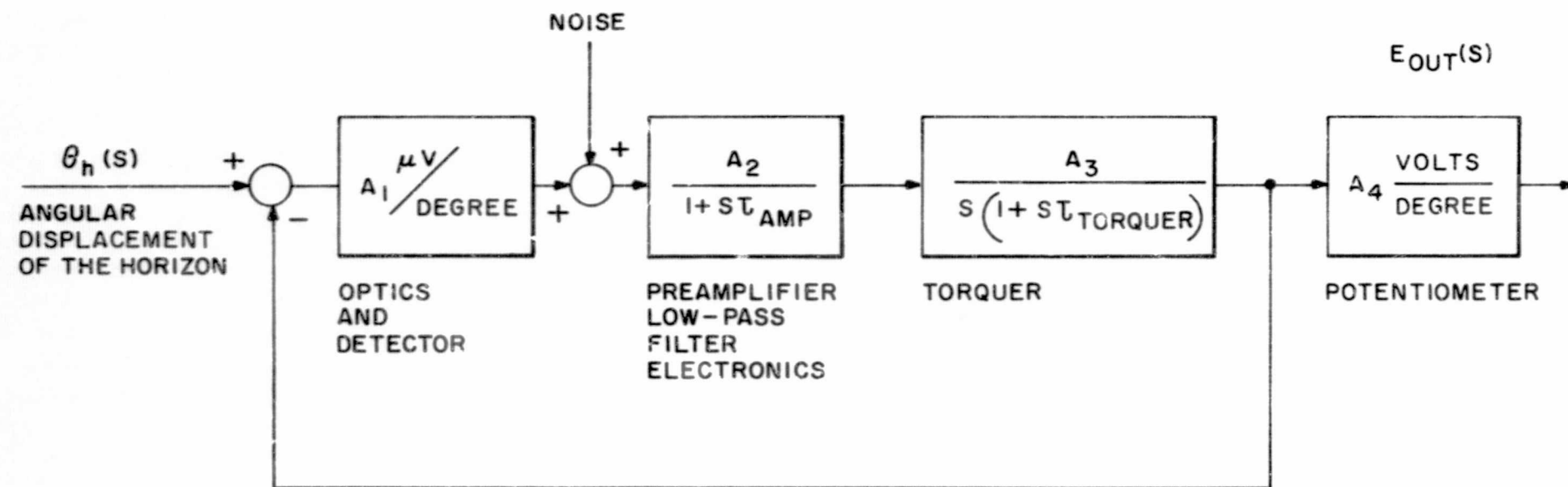


Figure A3-1 EDGE TRACKER SERVO BLOCK DIAGRAM

21801

The closed loop transfer function is obtained as:

$$\frac{E_{out}(S)}{\theta(S)} = \frac{A_1 A_2 A_3 A_4}{A_1 A_2 A_3 + S(1 + S \tau_{amp})(1 + S \tau_{torquer})}$$

To evaluate the limitation imposed on the system response by the mechanical characteristics of the torquer (and driven load inertia), set the electronics wide band:  $\tau_{amp} = 0$ . The denominator becomes a quadratic expression in s:

$$S^2 \tau_{torquer} + S + A_1 A_2 A_3$$

The natural frequency is

$$\omega_n = \sqrt{\frac{A_1 A_2 A_3}{\tau_{torquer}}}$$

and the damping ratio:

$$\zeta = \frac{1}{2} \frac{1}{\sqrt{A_1 A_2 A_3 \tau_{torquer}}}$$

With the electronics saturating for a one degree offset at a 10 volt level:

$$A_1 A_2 = 10 \text{ volt/degree}$$

A3 - 4

A<sub>3</sub> becomes the reciprocal of the back electromotive force of the torque motor. For the TQ18W torque motor of Aeroflex Laboratories

$$A_3 = \frac{1}{0.07} \frac{\text{radian}}{\text{volt-second}} = 820 \frac{\text{degrees}}{\text{volt-second}}$$

and

$$A_1 A_2 A_3 = 8200 \text{ second}^{-1}$$

The torquer time constant for the same motor is:

$$\begin{aligned} \tau_{\text{torquer}} &= \frac{\text{Rotor Inertia} \times \text{Winding Resistance}}{\text{Back EMF} \times \text{Torque to Current Ratio}} \\ &= \frac{0.00048 \text{ oz.in. sec}^2 \times 48 \text{ ohms}}{0.07 \text{ volts/rad/sec} \times 10 \text{ oz.in./amp}} \\ &= 33 \text{ milliseconds} \end{aligned}$$

Doubling the inertia to take into account the effects of the mechanical load, the effective time constant becomes:

$$\tau'_{\text{torquer}} = 66 \text{ milliseconds}$$

Thus the natural frequency

$$\omega_n = \sqrt{\frac{8200}{66 \times 10^{-3}}} = 352 \text{ radians/second}$$

and the damping ratio:

$$\zeta = \frac{1}{2} \frac{1}{\sqrt{8200 \times 66 \times 10^{-3}}} = 0.0215$$

The time  $T_r$  necessary to reach, for the first time, the position of equilibrium for this  $\omega_n$  and  $\zeta$  is taken from servo tables:

$$T_r = 4.8 \text{ milliseconds}$$

The damping of this system is clearly unsatisfactory and should be increased. Even then, a 10 millisecond response is possible as determined by purely mechanical considerations. This response is clearly much faster than the rate of motion, around any axis, of a space vehicle.

It is estimated that to get a 5:1 signal-to-noise ratio for the cold moon with a 1-inch diameter optics the required electronics time constant is 100 milliseconds larger than the torquer time constant.  $T_r$  due to this and the

required servo equalization should turn out to be of the order of 50 to 100 milliseconds, still considerably faster than normal space vehicle tumbling or roll rates.

Inland Motor Corporation manufactures a torquer, the T-1342, with a time constant of 20 milliseconds, an advantage over the Aeroflex torquer that is not fully utilizable, as the inertia of the load is larger than that of the torquer rotor.

#### A3.2 Field Switching Edge Tracker with Continuous Tracking Flat Mirror

In this section we will review the horizon sensor systems proposed in the Phase IA Study Report with particular emphasis on time constant trade-offs with sensitivity and accuracy. We will also show how tuning fork type vibrators may be used to accomplish the field switching which references the planet signal to outer space background. Several versions of such an edge tracker will be described, using several new concepts in executing the optical design.

The first system to be discussed is a version of the edge tracker described in Section 3.3.2.3.1 of the Phase IA Study Report.

Figures A3-2, A3-3, and A3-4 show three embodiments of this concept, in which either all reflecting or a combination of reflecting and refracting optics are used. In the case of the reflecting optics, a filter is required to define the optical passband. The detector uses a reflecting condensing cone. The reflecting cone serves as a field lens, placing an image of the primary optical collector on the detector. The same function could be served by a more standard field lens system or by an immersed thermistor or a combination of these elements. Chopping between fields at the planet's edge and a field in space  $10^\circ$  away from the planet edge is accomplished by means of a tuning fork vibrating chopper.

The first version shown in Figure A3-2 uses a scanning mirror to track the edge of the planet. The second and third versions are shown in a somewhat different arrangement, in which the objective lens along with the chopper and detector form a small optical assembly which is articulated by the action of the torquer and is thus made to track the edge of the planet.

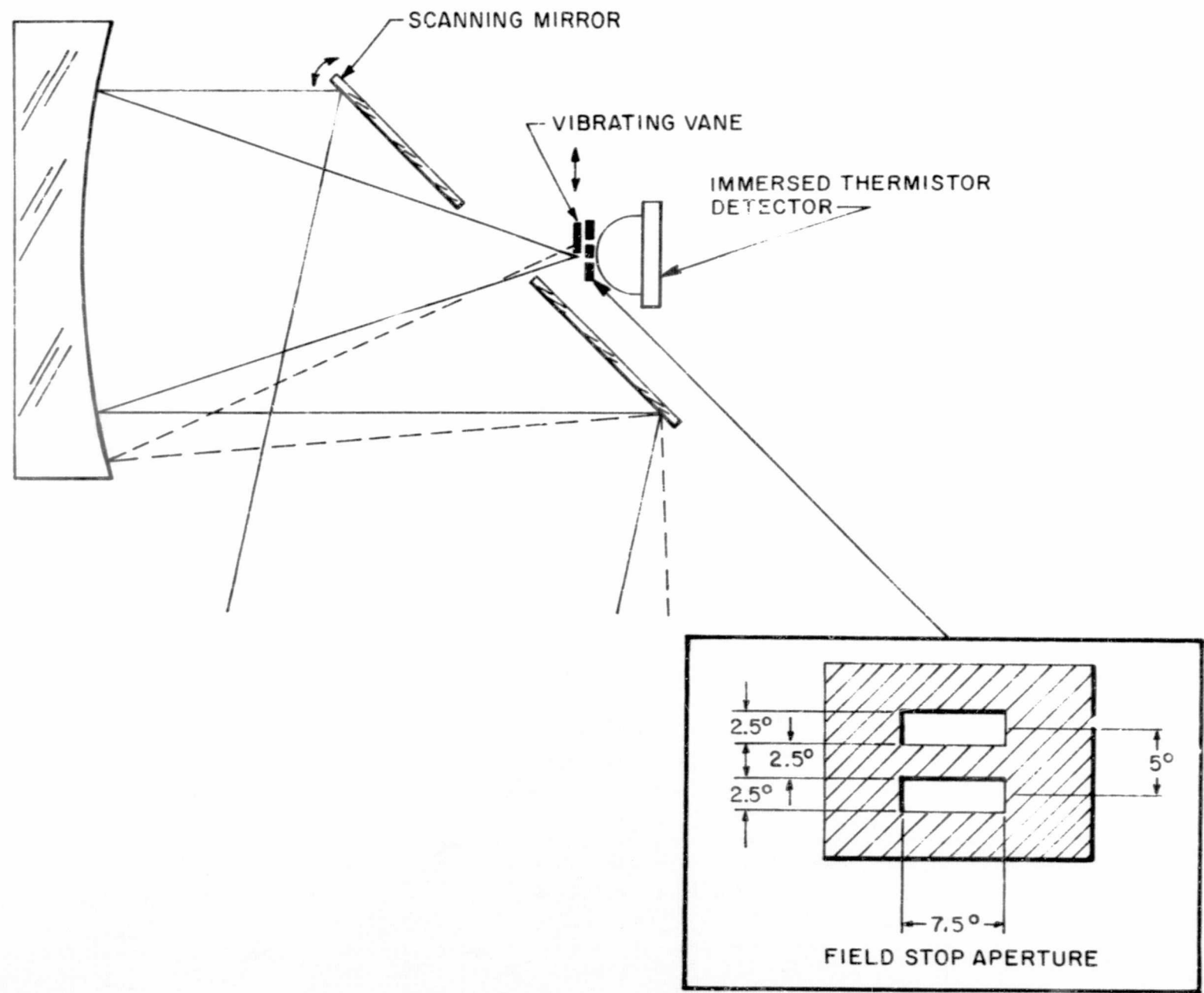
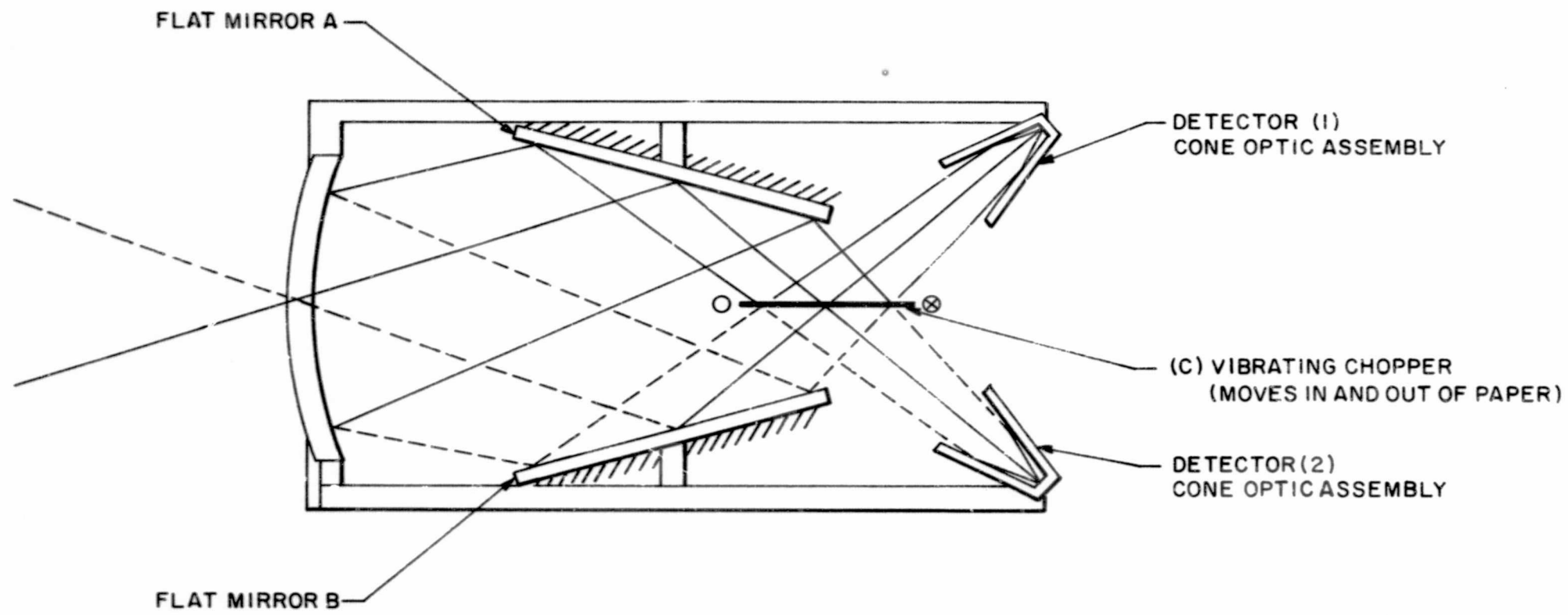


Figure A3-2 OPTICAL DRAWING OF FIELD SWITCHED EDGE TRACKER WITH CONTINUOUS TRACKING FLAT MIRROR 21802



21803

Figure A3-3 OPTICAL DRAWING OF EDGE TRACKER WITH SERVOED OPTICAL BARREL



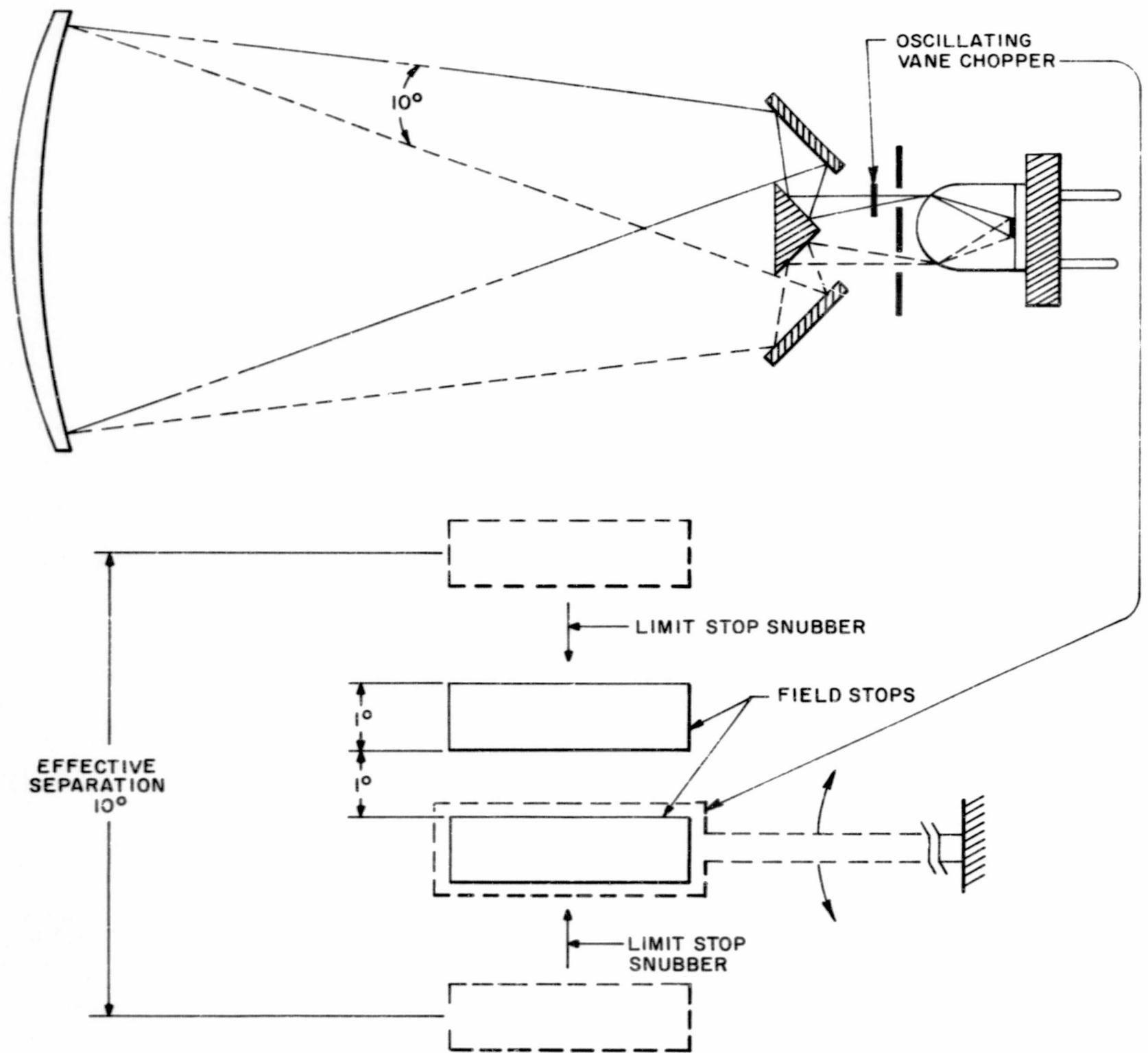


Figure A3-4 OPTICAL DRAWING OF EDGE TRACKER WITH REFLECTING PRISM FIELD RECOMBINATION

In Figure A3-2 we show an all-reflecting system which may use a spherical collector and a flat mirror to scan the image of the planet edge. The image is brought to a focus after the flat scanning mirror where a field stop aperture defines the fields of view of the system. Two identical rectangular cut-outs define fields separated in space by a field angle which may be made  $10^\circ$  if desired. A vibrating vane alternately opens and closes the two field stops, thus allowing the single detector to view in succession the field at the planet edge and an identical size reference field in outer space. As a result of the symmetry of this system, the detector sees a portion of the chopper vane and the field stop aperture at all times. This arrangement therefore does not result in aperture chop. All other elements which could give rise to signals from internal temperature differences are reflecting components and will therefore have extremely low emission. To define the spectral region of interest (20 to 40 microns), a filter will be placed at a convenient place in the system, such as the field stop aperture where only a small filter would be required. It may be desirable to use a

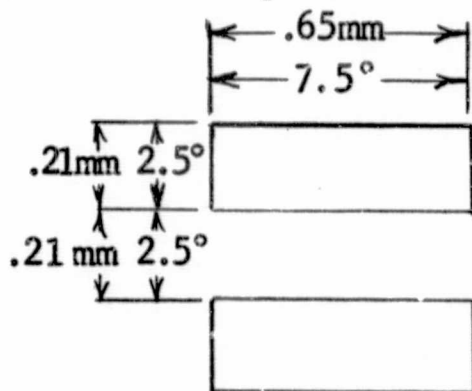
simple thin window, perhaps polyethylene, on the front aperture of the system simply as a dust cover.

In the system shown in Figure A3-2, we have used a 1-inch diameter, f/1 reflecting primary by way of example. A larger optical collecting system could be used to improve the system sensitivity if necessary. The chopper vane would be operated at a frequency of about 150 cps. The required movement of 2 mm can be easily provided by a Bulova tuning fork operating at this frequency.

The construction of the field stop is seen in the right-hand side of the sketch. It provides an instantaneous field of view of  $2.5^\circ \times 7.5^\circ$  and a separation of  $5^\circ$  between the space sensing and planet edge sensing fields. Greater separation can be provided, if desired, by deflecting the beam of radiation with auxiliary mirrors, as shown in Figure A3-4. In this manner, a different field of view can be easily provided. The field lens, immersed detector, or cone condensing optics image the primary optical element onto the detector through whichever aperture of the field stop happens to be opened at any instant of time through the action of the vibrating chopper vane.

The calculations for sensitivity and signal-to-noise ratio for this system based on a 1-inch diameter collector are shown below.

Assuming a 1-inch (25 mm) diameter aperture and an  $f/0.25$  optical speed due to detector immersion, the effective focal length is 6 mm. The focal length of the objective lens is 50 mm and the field stop has the angular and linear dimensions shown below.



To insure that all the focused rays passing through the above field stop reach the thermistor detector, the detector flake must subtend  $7.5^\circ \times 7.5^\circ$  or  $0.13 \times 0.13$  radian in combination with the effective focal length. The thermistor flake linear dimension is therefore  $0.13 \text{ radian} \times 6 \text{ mm} = 0.8 \text{ mm}$ , or the detector area,  $A = 0.8 \times 0.8 = 0.64 \text{ mm}^2$ .

For lunar irradiance completely filling one of the above  $2.5^\circ \times 7.5^\circ$  field stops, the power on the detector,  $P_D$ , is given by:

A3 - 14

$$\begin{aligned} P_d &= \Delta N_{(15-40)} \epsilon A_o \omega \\ &= 4 \times 10^{-5} \times 0.5 \times 5 \times 0.13 \times 0.043 \\ &= 0.5 \times 10^{-6} \text{ watts} \end{aligned}$$

The system NEP for a 1 cps output bandwidth =

$$6.3 \times 10^{-10} \sqrt{\frac{A}{T}} \times 5.6$$

where 5.6 is a degradation factor obtained as follows:

Amplifier noise factor	= 1.4
Detector bias reduction for high ambient temperature operation	= 1.4
Bolometer bridge factor	= 1.4
Chopping factor	= <u>2</u>
Total Degradation	= 5.6

$$\begin{aligned} \therefore \text{NEP} &= 6.3 \times 10^{-10} \sqrt{\frac{0.64}{2}} \times 5.6 \\ &= 2 \times 10^{-9} \text{ watts} \end{aligned}$$

The peak signal to rms noise ratio is therefore:

$$\frac{S}{N} = \frac{5 \times 10^{-7}}{2 \times 10^{-9}} = 250$$

This signal-to-noise ratio is based on a 1 cps bandwidth, the use of rms noise measurements, and the assumption of full illumination of a detector's field of view.

We must make the following corrections: Assume peak-to-peak noise of five times rms noise, assume that 20% of the detector is illuminated by the 90°K edge of the moon, and for the moment assume a 5-second integration time (bandwidth =  $1/2\pi 5 = 0.032$  cps).

The S/N becomes:

$$\frac{250 \times 0.2}{5 \times \sqrt{0.032}} = 54$$

Should it be required to increase the response time to provide a 100 millisecond preamplifier time constant, it will be necessary to correct the S/N ratio for the increased bandwidth. The correction is:

$$\left(\frac{S}{N}\right)_{\text{new}} = \left(\frac{S}{N}\right)_{\text{old}} \times \sqrt{\frac{\tau_2}{\tau_1}}$$

$$\left(\frac{S}{N}\right)_{\text{new}} = 54 \times \sqrt{\frac{0.1}{5}} \cong 8$$

This may be considered somewhat marginal. However, the figures used have been conservative throughout and it should be remembered that we can easily increase the aperture to a 2-inch diameter primary and thus gain a factor of two.

### A3.3 Field Switching Edge Tracker with Servoed Optical Barrel

Figure A3-3 shows another version of the edge tracker in which the reflecting primary is replaced by a lens. In this system, the entire optical unit is assembled in one tube which is mounted to a torquer and either rotated about the axis of the cylinder or moved in an arc anchored at the detector end of the tube. The optical arrangement is seen to be a symmetrical one in which a detector (shown by way of example as a cone condenser detector assembly) sees two fields separated by a pre-assigned fixed angle, depending on the angle of inclination of the flat mirrors A and B. The vibrating vane chopper (with reflecting surfaces on both sides of the vane) moves in and out of the paper.

When the chopper vane is positioned as shown in Figure A3-3, detector 1 sees energy entering the objective

lens reflected from flat mirror A and the top reflecting surface of chopper vane C. When the vane is moved out of the path of detector 1, energy enters the objective from a position  $10^\circ$  from that of the first phase, is reflected from mirror B, and enters detector 1. The field of view is defined by the detector size and the primary objective and its focal length. This arrangement, unlike that in Figure A3-2, requires a detector which need be only large enough to see one field of view (say  $2^\circ \times 2^\circ$ ). From the standpoint of sensitivity, this system has an advantage over that of Figure A3-2 because it can use a smaller detector with somewhat increased sensitivity, by a factor of  $\sqrt{3}$  because the detector can be  $1/3$  the size of the former.

In the sketch shown, a cone condenser detector is shown which is slightly less sensitive than the silicon immersed detector arrangement but has somewhat better spectral characteristics and is more suitable for use over a wider range of ambient temperatures than its immersion counterpart.

The detector sees the chopper vane at all times. Therefore, temperature variations of the blade do not produce



aperture chop. The only potential source of aperture chop is the possibility of differences in temperature or emissivity of the two flat mirrors. Since these will be in an isothermal environment and will have high reflectivity (gold surfaced), there is little danger of difficulty from this source. Errors due to differences in temperature or emissivity would be as computed on pages 3-87 and 3-88 of the Phase IA Study Report.

The second detector shown serves a twofold function. It is located so as to view fields displaced laterally about two degrees from the fields of detector 1. As such, it will provide an auxiliary error output signal in the event that the sun (or earth during a lunar mission) should appear in either field of detector 1. In addition, it becomes a redundant channel of information to provide increased reliability in the event that the first detector channel develops a fault.

In the arrangement shown, for a 1-inch diameter objective lens and the reflecting cone detector arrangement shown in Figure A3-3, the sensitivity and signal-to-noise ratio of this system is essentially the same as that presented in A3.2 above, assuming an equivalent field of view.

The basic difference in this arrangement and in the third system which follows is that these latter systems are arranged in an optical assembly which is positioned by the torquer to search and track the horizon edge. Although the mass and inertia of this arrangement of tracking optics is greater than that for the search mirror system shown in A3.2, both approaches are capable of fast response, as was shown in the introductory discussion on servo system response time.

#### A3.4 Field Switched Edge Tracker with Reflecting Prism Field Recombination

Figure A3-4 shows another arrangement of optics to obtain field switching through use of a vibrating vane chopper. This system uses flat mirrors and a reflecting prism to converge energy from regions separated by a conveniently chosen angle (e.g.,  $10^\circ$ ) to a field stop aperture which is made to subtend a much smaller angle at the detector and thus allows use of a smaller detector than may otherwise be required. For example, the fields may be displaced by  $10^\circ$  in space while the detector may be made to subtend  $3^\circ \times 3^\circ$  as shown in the sketch. The chopper vane in its harmonic motion opens one or another of the apertures of the field stop and thus allows

the detector to view more widely separated fields coming to a focus at the aperture alternately from the two sides of the prism. Through use of an immersion lens, field lens, or cone optics, the detector sees an image of the primary lens. In the example shown, the detector is square and receives energy from a field in space of  $1^\circ \times 3^\circ$ . If a different aspect ratio is desired, this may be provided by using a cylindrical field lens or a wedge immersion lens, etc.

Although not shown in the sketch of Figure A3-4, this system too may be provided with a second auxiliary sun-protect and redundant channel detector. This may be done by placing a reflecting chopper at a  $45^\circ$  angle and placing one detector in line with the incoming bundle of rays and the second detector in a vertical position to receive radiation reflected from the  $45^\circ$  reflecting elements.

Sensitivity of this system is once again similar to that calculated in Section 3.2 for comparable optics and fields of view, etc.

As in Section 3.3, this optical system may be assembled into a tube which is mounted to the torquer to obtain the required search and tracking function.

A4. ALL-ELECTRONIC EARTH/LUNAR HORIZON SENSOR SYSTEM

In the Phase IA Study Report, we examined the possibility of using the electronically sampled thermopile horizon sensing principle for the present earth/lunar horizon sensing mission. We concluded that the high accuracy required for the present application as compared to the LPHS (Lunar-Planetary Horizon Sensor) mission, for which a system is being designed under support from JPL, would make it necessary to either enlarge the optics or decrease the detector size. The latter step would require new detector development. In view of the superior accuracy and signal-to-noise ratio achievable with several other systems, this approach was not considered to be a very desirable one.

The possibility of a much faster response time requirement for the Earth/Lunar Horizon Sensor system reopens the question of whether possible modifications in the optics and detector arrangement may not make this approach worthwhile, particularly since the other systems which have been discussed suffer some loss in sensitivity due to the increased response time and bandwidth requirement.

Examining this system in more detail, we must first recognize the time constant limitations, even of this system. The detector time constant is approximately 100 milliseconds, so that even though we can readily arrange to sample detectors at a rate upwards of 1000 times a second, the individual detector will not respond to sudden changes in attitude at rates faster than its normal time constant. Also, we must remember that in its present form the output is essentially digital in form. If the fast response time desired is predicated on the need for rapid incremental changes which should be determined with high accuracy rather than due to possible abrupt and large changes in vehicle attitude, then the digital output may not provide the desired high accuracy, rapid correction signals.

Assuming that the nature of the output signal for this system is satisfactory, we can discuss the possible modifications which will be required. We will base our examination on the use of detector elements of the same size as used in the present engineering model. However, we will consider the use of bismuth tellurium junctions which provide a responsivity about five times higher than that of bismuth antimony

thermocouples. The resistance of the junctions for these new detectors is higher but is not considered to produce a serious increase in noise.

We will assume a modified optical system in which the focal length is increased from 5 cm to 25 cm, thus making the 0.9 mm width of each detector subtend  $0.2^\circ$ . The detectors may be made to subtend  $6^\circ$  in length, thus allowing use of three times as many junctions (63) as were used in the original detectors (21).

We can compute the expected signal levels and S/N by extrapolation from the original bismuth antimony thermopiles as follows:

Specific Responsivity  $\mathcal{R}' = 0.22$  volt/watt/cm<sup>2</sup> for a 21-junction bismuth tellurium detector (five times higher than for a 21-junction bismuth antimony thermopile).

Size of detector = 0.9 mm x 27 mm. We can build a detector of this size with 63 junctions.

Then  $\mathcal{R}' = 0.66$  volt/watt/cm<sup>2</sup>

The signal developed by the detector looking at a 90°K target which fills the field of view of that detector:

$$V_D = \frac{\pi}{4} \frac{\Delta N R' \epsilon}{f^2}$$

where  $\Delta N_{20-40\mu}$  for 90°K =  $4 \times 10^{-5}$

the efficiency,  $\epsilon = 0.5$

assume an f/3.5 system

$$V_D = \frac{\pi}{4} \frac{4 \times 10^{-5} \times 0.66 \times 0.5}{(3.5)^2} = 0.85 \text{ microvolt}$$

Resistance of the 63-junction thermopile is expected to be about 120K ohms (which poses some difficulties for a switching system).

If drift constitutes the lower limit of operation for the system, a one microvolt level may be assigned to such fluctuations over the ambient operating temperature variations and the signal to drift level becomes 0.85, which is clearly inadequate.

The system we require will have to have at least  $20^\circ$  acquisition capability in order to function for the desired altitude range and attitude deviations. For the  $0.2^\circ$  subtense, we will therefore require 100 detectors for each axis and each will subtend  $6^\circ$  in length.

An optical arrangement for such a system without use of folding is shown in Figure A4-1.

Insofar as the dimensions and weight of such a unit are concerned, we have considered a scaling-up of the focal length. If the detectors were placed at a distance of 25 cm from the spherical reflector, the aperture of the system and the offset heat source would have to be placed at the center of curvature, at 50 cm from the collector. This implies an optical barrel of 20-inch length. The weight increase for such a system is estimated to be by a factor of ten. For a magnesium casting, the weight per head is probably going to be of the order of 35 pounds.



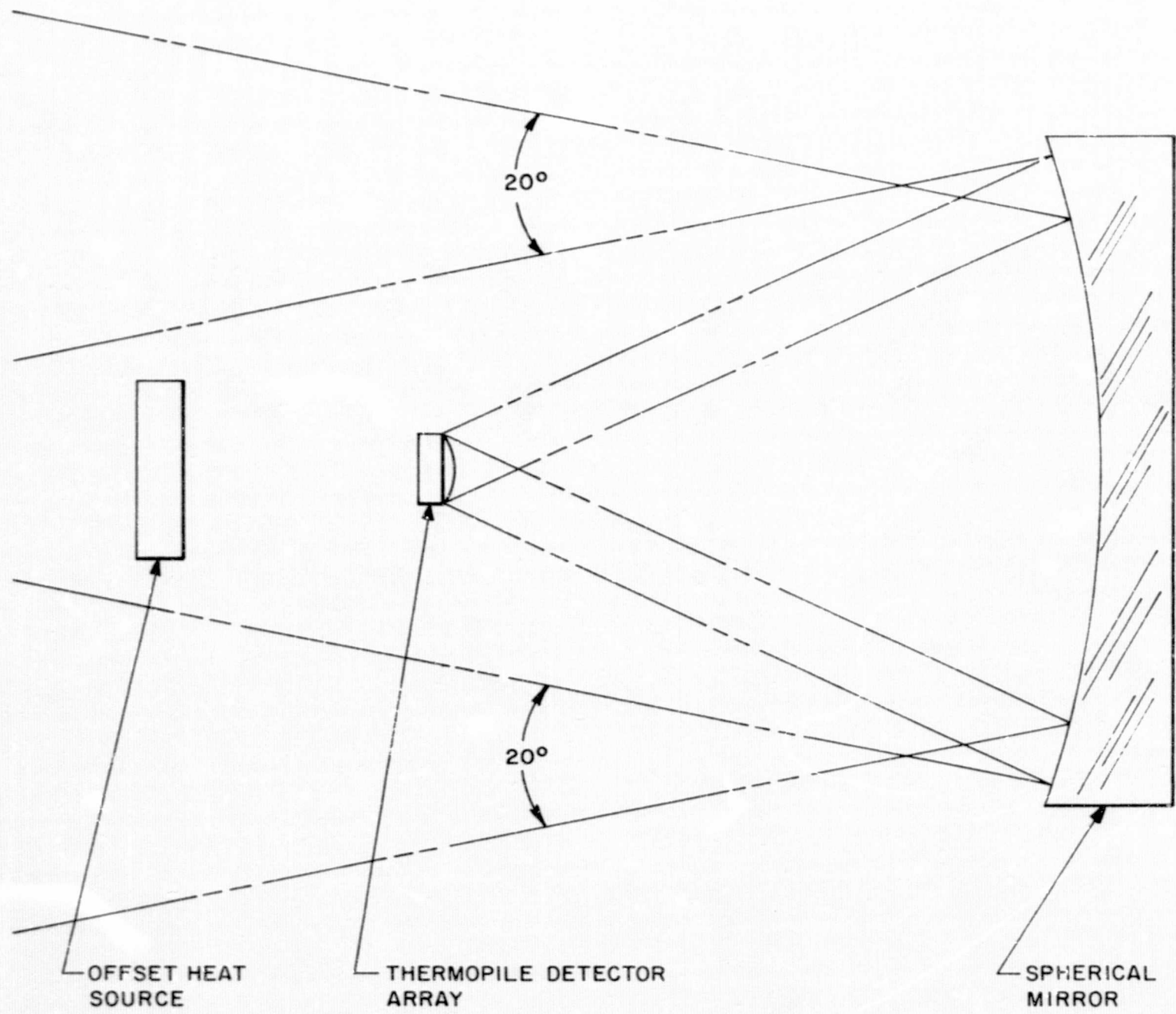


Figure A4-1 OPTICAL DRAWING OF ALL ELECTRONIC MULTIELEMENT THERMOPILE HORIZON SCANNER

21805

A5. CONCLUSIONS AND RECOMMENDATIONS

A5-1 Field Switched Edge Tracking Horizon Sensors

From the foregoing discussions, it is evident that the system which offers the best prospects of meeting the design goals for the Earth/Lunar Horizon Sensor System, including a possible large speed-up of response time, continues to be the field switched edge tracker. This deduction is based on facts set forth in the Phase IA Study Report, backed up in this Addendum by a review of the servo response time expectations and some trade-off calculations of the signal-to-noise ratio changes which result when the response time specified is much faster than was considered appropriate in the original study report.

Our calculations show that a 20 millisecond response time is not out of the question for the small servoed optical elements, though it is not considered probable that such response times will be required in view of the fact that the rate of attitude variations of the spacecraft with its far greater mass and inertia is not likely to approach these time constants. Calculations also show that the field switched edge tracker

also provides a considerably better signal-to-noise ratio and accuracy capability than the other systems considered and appears to have the required minimal sensitivity even for a 20 millisecond response time system.

We therefore favor the field switched edge tracker in the form discussed in Section A3.2 and believe that it can be implemented within the scope of the present program, on a schedule as discussed in early conversations with NASA/MSD personnel (i.e., a 2-month detail design study and an 8-month program of engineering, fabrication, checkout, and evaluation.

#### A5.2 Indexed Edge Tracking Horizon Sensors

The various indexed edge trackers discussed in Section A2 have certain advantages but also have some limitations which must be kept in mind. Among the advantages, we can cite the fact that the indexing movement itself is operated only at times when large attitude or altitude changes are encountered. Such intermittent operation leads to a long life expectancy for the indexing mechanism, which may be operated in a vacuum environment without requiring lubrication. Electrical power for the indexing mechanism will be required

principally during the course of stepping to a new index position, the standby power being negligibly small.

Insofar as the response time is concerned, however, the situation is more complex. If the fast response time requirement is predicated on the need for high accuracy and a rapid, smooth reaction to disturbances, then the indexing and sampling system may not be the best answer. In these systems, the error signals are obtained essentially in digital form in discrete steps rather than as a smooth transfer characteristic. The signal-to-noise ratios of the systems described also appear to be marginal for 90°K lunar temperatures and are considerably lower than for the field switched edge trackers. On the whole, size, weight, and power requirements will be similar to those of the field switched edge trackers.

#### A5-3 All-Electronic Horizon Sensors

From the standpoint of signal-to-noise ratio, the electronically sampled thermopile horizon sensor for lunar applications requiring a 0.1° attitude sensing capability is clearly inadequate and inferior to the other systems

considered. A higher signal-to-noise or drift ratio may be obtained by increasing the dimensions of the optical collector system. However, the size and weight of the system, as discussed in Section A4, already are above those specified as the design goals for the Earth/Lunar Horizon Sensor System. Unless the requirements for accuracy (particularly for the case of lunar applications) are released, we could therefore not recommend this approach at the present time.

TABLE A5-1 Comparison of Sensitivity, Accuracy, and Response Time of Various Horizon Sensor Systems

Paragr. in Text	System Type	Signal-to-Noise Ratio for 0.1° Accuracy on a 90°K Target	Response Time	Optics Diameter	Remarks
A2.2	Single Detector, Linear Scan, Indexing	5:1	75 msec	2"	Does not provide smooth error transfer characteristic. Output consists of digits or steps.
		5:1	300 msec	1"	
A2.3	Field Switching, Five Thermistor Detectors, Indexing	4.8:1	100 msec	2"	Does not provide smooth error transfer characteristic. Output consists of digits or steps.
A2.4	Field Switching, Five Thermopile Detectors, Indexing	3:1	100 msec	2"	Does not provide smooth error transfer characteristic. Output consists of digits or steps.
A3.2	Field Switched Edge Tracker, Continuous Tracking, Flat Mirror	8:1	50-100 msec	1"	Response determined by servo stability requirements.
		54:1	5 seconds		
A3.3	Field Switched Edge Tracker, Servoed Optical Barrel	8:1	50-100 msec	1"	Response determined by servo stability requirements.
		54:1	5 seconds		
A3.4	Field Switched Edge Tracker, Reflecting Prism Field Recombination	8:1	50-100 msec	1"	Response determined by servo stability requirements.
		54:1	5 seconds		
A4	All-Electronic System	0.85:1	100 msec	13 cm <sup>2</sup>	Long focal length (25 cm); offset heat source needed: